

PROJECT #2016-026

DATE: May 9-10, 2016

In Situ Performance Verification of Geogrid-Stabilized Aggregate Layer: I8 near El Centro, CA

By

David J. White, Ph.D., P.E. (IA)

Ingios Geotechnics, Inc.



Prepared for Tensar International Corporation, Alpharetta, GA

List of Notations and Abbreviations

APLT	Automated plate load testing
B	Width of footing for a square plate and diameter of footing if circular
B_1	Side dimension of a square plate used in load test or diameter of a circular plate
C	Plastic deformation after the first cycle of repeated loading
CBR	California bearing ratio
CL	Low plasticity clay
d	Scaling exponent
DCP	Dynamic cone penetrometer
DPI	Dynamic penetration index
E_v	Strain or deformation modulus
f	Shape factor
$F_{Bending}$	Correction factor for plate bending
$F_{PlateSize}$	Correction factor for plate size
$F_{Saturation}$	Correction factor for future saturation
FWD	Falling weight deflectometer
h	Thickness of the top layer (in layered analysis)
h_e	Equivalent thickness (based on Odemark's MET concept)
$k1^*, k2^*, k3^*$	Stress-dependent resilient modulus model parameters
MET	Method of equivalent thickness
$M_{r-comp.}$	Composite resilient modulus
M_{r-SG}	Subgrade resilient modulus
M_{r-Base}	Base layer resilient modulus
M_{r1}	Resilient modulus of the top layer (in layered analysis)
M_{r2}	Resilient modulus of the bottom layer (in layered analysis)
N	Number of loading cycles

N^*	Loading cycle number at which the application of additional cyclic loadings results in very low accumulation of additional permanent deflection
P	Cyclic load
r	Radius of plate
$\Delta\sigma_p$	Cyclic stress
δ_p	Permanent deformation
$\Delta\delta_p$	Change in permanent deformation
δ_r or $\delta_{r=0}$	Resilient deflection at edge of the plate
$\delta_{r,r'}$	Resilient deflection at distance r' away from the plate center
ν	Poisson ratio
ν_1	Poisson ratio of the top layer (in layered analysis)
ν_2	Poisson ratio of the bottom layer (in layered analysis)

Executive Summary

At the request of Tensar Corporation, Ingios Geotechnics, Inc. conducted automated plate load tests (APLTs) on Interstate 8, between Bonds Corner Road and S33, east of El Centro, California on May 9-10, 2016. The purpose for performing cyclic APLTs was to determine composite, base layer, and subgrade layer resilient modulus (M_r) values. The focus of the testing program was to evaluate the pavement foundation consisting of nominal 6 in. of recycled concrete aggregate (RCA) base (SW-SM with 5.0 percent fines content) stabilized with TX160 multi-axial geogrid with hexagonal structure and triangular apertures.

Field testing consisted of eight APLTs involving six different applied cyclic stresses. Additionally, APLT deflection basin measurements at three positions extending away from the center of the plate (2r, 3r, and 4r), and two extended cycle (5000+ cycles) APLTs at different stress levels were performed. Dynamic cone penetration tests (DCP) were performed at each test point to characterize the vertical penetration resistance profile.

The test results were used to determine the in situ "universal" model (AASHTO 2015), the k_1^* , k_2^* , and k_3^* model parameters for the composite, aggregate base and subgrade layers. Analysis of permanent deformation model parameters (C and d), the number of cycles (N^*) to achieve near-linear elastic δ_p rate limit, δ_p at N^* , and number of cycles (N) to achieve a $\delta_p = 0.05$ to 0.1 in. deformation were used to describe the stress versus cycles behavior.

The composite test results exhibited a decrease in modulus with increasing cyclic stress. This decrease in modulus is a characteristic of composite behavior with aggregate base over softer subgrade soils. Box plot and descriptive statistics for all in situ M_{r-comp} values provide an assessment of the variability and trend in composite modulus with increasing cyclic stress.

Using the "universal" model (AASHTO 2015), the k_1^* , k_2^* , and k_3^* model parameters averaged 1,384.9, -0.190, and 0.495, respectively, and are in-line with what would be expected for laboratory determined values. On average, the measured M_{r-comp} versus predicted composite resilient modulus ($M_{r-comp} (pred.)$) showed a standard error of about 2.7%, suggesting that the

model parameters provide a statistically significant and quality fit to the experimental data.

Layered elastic analysis accounting for stress at the subgrade layer shows that M_{r-Base} values ranged between 40.9 ksi and 65.8 ksi, while the M_{r-SG} values ranged between 4.4 ksi and 12.7 ksi. k_1^* , k_2^* , and k_3^* model parameters averaged 3,075.7, 0.112, and -0.085, respectively for the aggregate base layer and 685.8, -0.182, and -0.185, respectively for the subgrade layer.

Analysis of permanent deformation (δ_p) and deformation scaling exponents (d) for each load step shows that the permanent deformation increased with increasing cyclic stress, as expected. Modeling permanent deformation response of each load step showed that at cyclic stresses less than about 20 psi typically exhibited a near-linear elastic behavior during loading.

Two extended cycle APLTs (5000+ cycles) were performed at two different cyclic stresses (8.5 psi and 18.2 psi) on the aggregate base layer to determine the composite permanent deformation model parameters (C and d), the number of cycles (N^*) to achieve near-linear elastic δ_p rate limit ($\Delta\delta_p/\text{cycle} = 1\text{E-}06$ in./cycle), δ_p at N^* , and number of cycles (N) to achieve a $\delta_p = 0.05$ to 0.1 in. Results demonstrate that N^* ranged from 2.1k to 2.2k cycles for the two tests. The N value to reach $\delta_p = 0.05$ in. at $\sigma_{\text{cyclic}} = 8.5$ psi is estimated at 4.7 million cycles while at $\sigma_{\text{cyclic}} = 18.2$ psi it is about 84k cycles.

DISCLAIMER:

Ingios Geotechnics, Inc. and its Affiliates disclaim any and all responsibility and liability for the use of any such data, information and/or the analysis presented in this report. Although Ingios Geotechnics, Inc. takes all possible care to ensure the correctness of published information, no warranty can be accepted regarding the correctness, accuracy, uptodateness, reliability and completeness of the content of this information.

Ingios Geotechnics, Inc. expressly reserves the right to change, to delete or temporarily not to publish the contents wholly or partly at any time and without giving notice. Liability claims against Ingios Geotechnics, Inc. because of tangible or intangible damage arising from accessing, using or not using the published information, through misuse of the contents or as a result of technical breakdowns are excluded.

Contents

List of Notations and Abbreviations.....	ii
Executive Summary	iv
1 Introduction	1
1.1 Background	1
1.2 Objective	2
1.3 Scope.....	2
2 Test Methods.....	3
2.1 Automated Plate Load Test (APLT)	3
2.1.1 <i>Composite Resilient Modulus</i>	5
2.1.2 <i>Layered Analysis</i>	9
2.1.3 <i>Permanent Deformation Monitoring</i>	12
2.2 Dynamic Cone Penetration (DCP) Testing	13
2.3 Laboratory Testing.....	14
3 Experimental Study.....	16
3.1 Field Experimental Study.....	16
3.2 Project Details	17
4 Results.....	21
4.1 Dynamic Cone Penetration (DCP) Test Results.....	21
4.2 In Situ Composite Resilient Modulus.....	21
4.3 Layered Analysis.....	24
4.4 Forecasting Trafficking Performance	27
5 Summary.....	28
References.....	30
Appendix: APLT and DCP Test Results and Analysis.....	33

Figures

Figure 1. APLT test system used on I-8 project.....	4
Figure 2. Example APLT setup for real-time test monitoring including control panel, display and plate assembly.	4
Figure 3. Illustration of the parameters measured from APLT cyclic plate load tests.	5
Figure 4. APLT test setup with deformation measurements obtained at $2r$ and $3r$ from the plate center axis.	6
Figure 5. Deflection basis measurement kit positioned at $2r$, $3r$, and $4r$ positions (where ‘ r ’ is the radius of the plate) from the plate center axis.....	9
Figure 6. Illustration of Odemark’s MET concept.	11
Figure 7. DCP test on aggregate base layer.....	14
Figure 8. In situ APLT test locations on May 9-10, 2016 on I-8 near El Centro, California.	17
Figure 9. Compacted recycled concrete aggregate (RCA) over TX160 geogrid (May 9, 2016).....	18
Figure 10. APLT testing at Sta. 2726+00 (May 9, 2016).	18
Figure 11. (top) Full recycled concrete aggregate (RCA) gradation sample and (bottom) material retained on No. 4 sieve after washing and oven-drying (May 10, 2016 sample).....	19
Figure 12. Grain-size analysis and classification of recycled concrete aggregate (RCA) base (sampled May 9, 2016).	20
Figure 13. Box plot (top) and descriptive statistics (bottom) for all in situ composite resilient modulus tests for six cyclic stress values.	24

Tables

Table 1. Summary of typical ranges of laboratory k_1 , k_2 , and k_3 parameters from NCHRP (2004b), results from recent studies and values from this project.....	8
Table 2. Summary of plate tests and configurations.....	16
Table 3. Summary geogrid material mechanical properties.	16
Table 4. Summary of project location and notes.....	17
Table 5. Comparison of in situ M_{r-comp} and permanent deformation results for 12 in. plate APLT tests for the last applied stress sequence ($\sigma_{cyclic} = 38.5$ psi).	22
Table 6. Comparison of “universal” model regression parameters for in situ M_{r-comp} , break point cyclic stress, and predicted in situ M_{r-comp} at break point stress.....	23
Table 7. Comparison of in situ M_{r-comp} , M_{r-Base} , and M_{r-SG} results for 12 in. plate APLT tests for the last applied stress sequence ($\sigma_{cyclic} = 38.5$ psi).	25
Table 8. Comparison of “universal” model regression parameters for in situ aggregate base layer, M_{r-Base}	26
Table 9. Comparison of “universal” model regression parameters for in situ subgrade layer, M_{r-SG}	26
Table 10. Summary of permanent deformation prediction parameters.	27

1 Introduction

1.1 Background

The static plate load test (AASHTO T222) has been used in different geotechnical engineering fields and particularly in the characterization of foundation layer properties for rigid pavements. The strain or deformation modulus (E_v) is commonly used in pavement design in Europe, while the resilient modulus is used in the U.S. The strain modulus, E_{v2} is calculated from the second loading cycle using the Boussinesq solution and secant method (DIN 18134, 2001). In contrast, resilient modulus (M_r) is determined using *resilient* deflection of materials after many stress cycles. Resilient modulus can be obtained from the laboratory triaxial test (e.g., per AASHTO T307, 2000 or NCHRP, 2004). However, due to the complexity of the laboratory triaxial test and often non-representative boundary conditions, the resilient modulus of pavement foundation materials is often obtained from empirical correlations between resilient modulus and other properties such as soil classification, California Bearing Ratio (CBR) or Hveem R-value.

In situ resilient modulus is also predicted from non-destructive surrogate tests including the falling weight deflectometer (FWD) or light weight deflectometer (LWD). In practice, elastic moduli values calculated from these test devices based on *elastic* deformations are often confused with resilient modulus values which is based on *resilient* (i.e., recoverable) deformations.

One of the major limitations of these non-destructive surrogate tests is the lack of a conditioning stage prior to testing. During pavement construction, pavement foundation materials are subject to relatively high loads from construction traffic and compaction equipment. In response to these loads, aggregate particles rearrange themselves resulting in higher density and stiffness. For mechanically stabilized layers (i.e., those including a geogrid), this results in greater particle to particle interlock leading to aggregate confinement and particle immobilization. For this reason, it is important to apply conditioning load cycles prior to testing to determine in situ resilient modulus. Once surface paving is complete, the pavement foundation below is confined by the overlying pavement layers. The response of a pavement foundation to subsequent repeated traffic loading is both nonlinear and

stress-dependent, therefore the effect of confinement is an important condition to consider in a field based resilient modulus test. In response to this need, the Automated Plate Load Test (APLT) system was designed to directly measure the influence of load cycles and confining pressure on in situ resilient modulus measurements and permanent deformation of the pavement foundation.

1.2 Objective

The objective of this study was to conduct cyclic APLTs to determine in situ M_r and deformation characteristics of the mechanically stabilized aggregate base and subgrade foundation layers. The road test section consisted of an aggregate base course layer (crushed recycled concrete aggregate (RCA), stabilized with TX160 multi-axial geogrid. The TX160 multi-axial geogrid has a hexagonal structure and triangular apertures.

1.3 Scope

Cyclic APLTs were performed using a 12 in. diameter plate at eight test locations using 1,100 cycles, which included a 500 cycle conditioning step followed by six 100 cycle loading steps with increasing stress for each step. The maximum stresses for the six loading steps were 5, 10, 15, 20, 30, and 40 psi. The maximum stress for the conditioning step was 15 psi. A 0.2 sec. load pulse followed by a 0.8 sec. dwell time was selected for testing. Plate deflections were monitored and a sensor kit was installed to measure ground deflections at selected radial distances (2 x and 3 x radius) from the plate center. Results were used to determine composite, base layer, and subgrade layer M_r values.

In addition, extended cyclic APLTs between 5,000 to 6,000 cycles were conducted at two test locations using 8.5 psi or 18.2 psi cyclic stress. These tests were conducted to predict long-term trafficking performance.

Dynamic cone penetration tests (unconfined surface) were performed at each test location to determine penetration resistance and CBR profiles up to a depth of about 2.5 ft below surface. Photographs documented the surface conditions. Results were used to evaluate performance of the TX160 geogrid stabilized road section.

2 Test Methods

2.1 Automated Plate Load Test (APLT)

For rapid field assessment of critical performance parameters, Automated Plate Load Test (APLT) equipment was developed by Dr. David J. White (U.S. and International Patents Pending). The APLT equipment was specifically developed to perform rapid field testing of pavement foundations, embankments, and stabilized materials. The APLT equipment is capable of measuring:

- Modulus of subgrade reaction
- Confining stress dependent resilient modulus
- Strain modulus
- Permanent deformation
- Bearing capacity
- Undisturbed tube sampling and extrusion
- Shear wave velocity/modulus
- Cone penetration testing
- Borehole shear testing
- Rapid in situ permeability

Figure 1 shows the plate load test equipment mounted on a trailer unit and Figure 2 provides an example of the automated load pulse and deflection output provided to the operator. The results of cyclic deformation, permanent deformation, elastic modulus, stiffness, resilient modulus, cyclic stresses, and number of cycles are calculated in real-time and are available for reporting immediately (see illustration of key parameters in Figure 3). The APLT unit is automated using electric-hydraulic control systems.



Figure 1. APLT test system used on I-8 project.

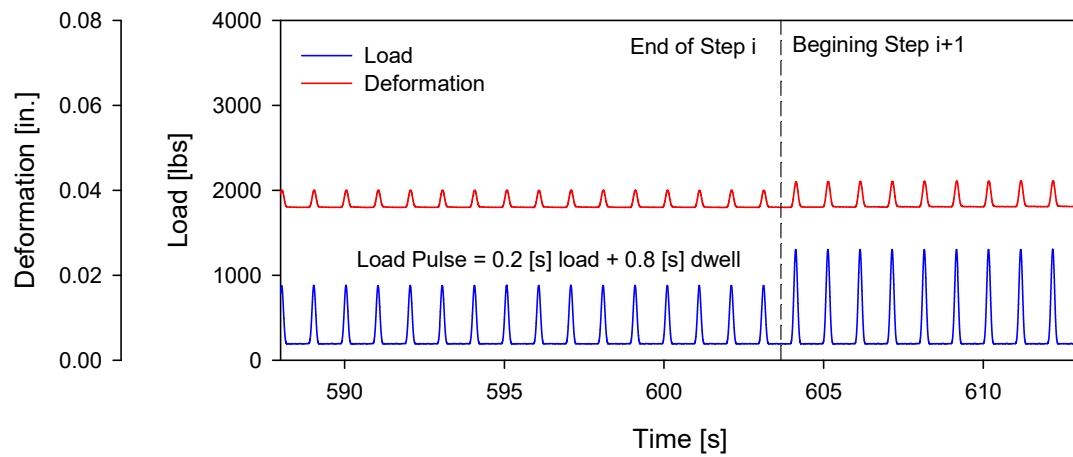


Figure 2. Example APLT setup for real-time test monitoring including control panel, display and plate assembly.

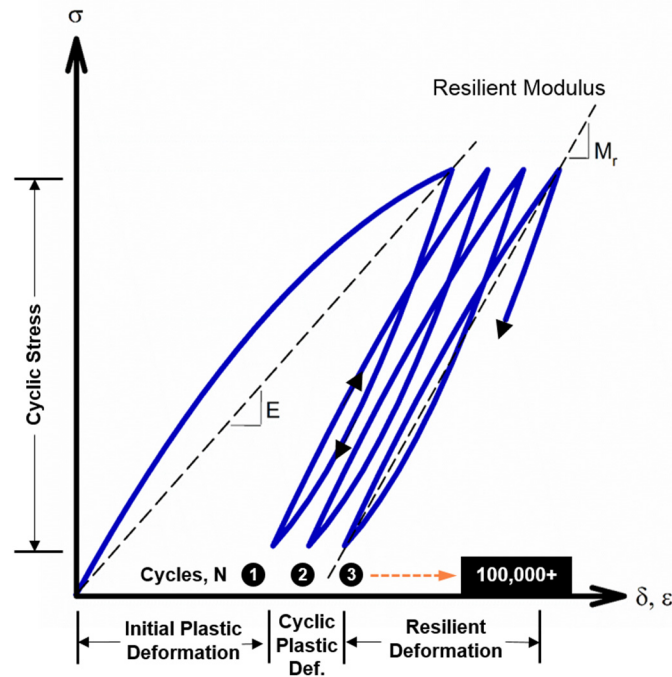


Figure 3. Illustration of the parameters measured from APLT cyclic plate load tests.

2.1.1 Composite Resilient Modulus

The in situ composite M_r is calculated as the ratio of the cyclic stress divided by the resilient deflection (during unloading) using the Boussinesq's half-space equation:

$$M_{r-comp} = \frac{(1 - \nu^2) \cdot \Delta\sigma_p \cdot r}{\delta_r} \times f \quad (1)$$

where,

M_{r-comp} = in situ composite resilient modulus (uncorrected),

δ_r = the resilient deflection of plate during the unloading portion of the cycle (determined as the average of three measurements along the plate edge, i.e., at a radial distance $r' = r$),

ν = Poisson ratio (assumed as 0.40),

$\Delta\sigma_p$ = cyclic stress,

r = radius of the plate,

f = shape factor selected as 8/3 for rigid plate on granular material.

In reality, Poisson's ratio will vary between test sections due to the aggregate stabilization mechanism(s) and loading conditions. Several papers in the literature demonstrate that this value can vary from 0.1 to 1+ due to the stress level and volume change characteristics (e.g., Brown et al. 1975, LeKarp et al. 2000).

Corrections to the measured in situ composite M_r can be made as shown in Eq. (2) for plate bending ($F_{Bending}$) and the effect of future saturation ($F_{Saturation}$) in the subgrade:

$$M'_r = \frac{(1-\nu^2) \cdot \Delta\sigma_p \cdot r}{\delta_r} \times f \times F_{Bending} \times F_{Saturation} \quad (2)$$

In this report, no corrections were made for plate bending (i.e., $F_{Bending}$ is assumed as 1). The 12 inch diameter plate used in this study was 1 in. thick with a 6 in. diameter plate that is 1 in. thick and a carriage plate as shown in Figure 4. Further, no corrections were applied for future saturation conditions (i.e., $F_{Saturation}$ is 1).



Figure 4. APLT test setup with deformation measurements obtained at $2r$ and $3r$ from the plate center axis.

The M_r parameter is a stress-dependent parameter. In general, most soils exhibit the effects of increasing stiffness with increasing bulk stress and decreasing stiffness with increasing shear stress (Andrei et al. 2004). The APLT testing program was designed to assess the in situ composite resilient

modulus at six different stress levels. The results were used to model the behavior using the “universal” model (AASHTO 2015) shown in Eq. (3):

$$M_r = k_1^* P_a \left(\frac{\theta}{P_a} \right)^{k_2^*} \left(\frac{\tau_{oct}}{P_a} + 1 \right)^{k_3^*} \quad (3)$$

where,

M_r = in situ resilient modulus (psi);

P_a = atmospheric pressure (psi);

θ = bulk stress (psi) = $\sigma_1 + \sigma_2 + \sigma_3$ = applied cyclic stress (σ_{cyclic}) for M_{r-comp} calculations because there is no confining stress at the surface;

$\sigma_2 = K_o \sigma_1$;

$\sigma_3 = \sigma_2$

K_o = coefficient of lateral earth pressure at rest = $\nu/(1-\nu)$;

ν = Poisson’s ratio assumed as 0.4;

τ_{oct} = octahedral shear stress (psi) = $\sqrt{(\sigma_1 - \sigma_2)^2 + (\sigma_2 - \sigma_3)^2 + (\sigma_3 - \sigma_1)^2} / 3$; and

k_1^* , k_2^* , and k_3^* = regression coefficients determined from in situ testing (these coefficients are presented herein with a * to differentiate with the regression coefficients traditionally developed using laboratory test results).

Bulk stress, octahedral shear stress, and measured composite resilient modulus values from the last five load cycles in each loading sequence were used in the data analysis. The k_1^* coefficient is proportional to M_r and therefore is always > 0 . The k_2^* coefficient explains the behavior of the material with changes in the bulk stresses. Increasing bulk stress increases the M_r value and therefore the k_2^* coefficient should be ≥ 0 . The k_3^* coefficient explains the behavior of the material with changes in shear stresses. Increasing shear stress softens the material and decreases the M_r value. Therefore the k_3^* coefficient should be ≤ 0 .

Based on laboratory test results, NCHRP (2004b) summarized typical values for k_1 , k_2 , and k_3 parameters for granular and non-granular materials compacted to different densities and moisture contents relative to optimum moisture contents. Table 3 provides a summary of the typical ranges from

laboratory tests for granular base, granular subgrade, and non-granular subgrade materials. In comparison, the range of k_1^* , k_2^* , and k_3^* values measured in situ for this project and a similar project conducted in 2015 (White et al. 2015) are similar.

Table 1. Summary of typical ranges of laboratory k_1 , k_2 , and k_3 parameters from NCHRP (2004b), results from recent studies and values from this project.

Materials	k_1	k_2	k_3
Granular base (A-1-a and A-1-b)*	560 to 3,417	1.021 to 1.431	-1.753 to -0.571
Granular subgrade (A-4)*	151 to 4,288	0.132 to 1.121	-3.785 to +0.165
Non-granular subgrade (A-6)*	246 to 5,480	-0.077 to 0.617	-3.690 to +1.538
APLT composite granular base over subgrade (White et al. 2015)	611 to 2,319	-0.009 to 1.261	-6.792 to +0.192
Brown Field Airport Project: Composite A-1-a granular base stabilized with TX5 or TX7 geogrid over subgrade (White 2016)	1,005 to 1,252	-0.101 to 0.240	-2.829 to 0.974
Brown Field Airport Project: A-1-a granular base stabilized layer with TX5 or TX7 geogrid (White 2016)	1,415 to 1,906	-0.176 to 0.264	-2.856 to 1.845
Brown Field Airport Project: SP-SM subgrade layer (White 2016)	674 to 966	-0.004 to 0.284	-4.870 to -1.121
This project: Composite A-1-a granular base stabilized with TX160 over subgrade	1,041 to 1,822	-0.258 to -0.050	-0.185 to 1.299
This project: A-1-a stabilized layer with TX160	1,725 to 4,438	-0.321 to 0.669	-3.172 to 2.722
This Project: CL subgrade layer	321 to 952	-0.323 to -0.001	-2.090 to 1.869

*per NCHRP report, specimens compacted wet to dry of optimum moisture contents

Results from past testing on granular base material over subgrade (White et al. 2015) indicated that the M_{r-comp} increased with cyclic stress up to a certain stress level and then decreased. The cyclic stress at which the peak M_{r-comp} was observed is referred to herein as the break-point cyclic stress ($\sigma_{cyclic-BP}$). Based on the relationship between the k_1^* , k_2^* , and k_3^* parameters and M_{r-comp} , the $\sigma_{cyclic-BP}$ and the corresponding break-point composite resilient modulus ($M_{r-comp(pred.)-BP}$) were determined.

2.1.2 Layered Analysis

Individual subgrade and base layer resilient modulus values were determined by obtaining resilient deflections measured at radii of 12 in. ($2r$), 18 in. ($3r$), and 24 in. ($4r$) away from the plate center. The test setup is shown in Figure 5. The layered analysis measurement system was developed specifically for testing unbound materials and provides average resilient deflections measured over one-third (60 degrees) of the circumference of a circle at the selected radii. This method was designed to improve practices that use point measurements, which are often variable from point-to-point for unbound aggregate materials.

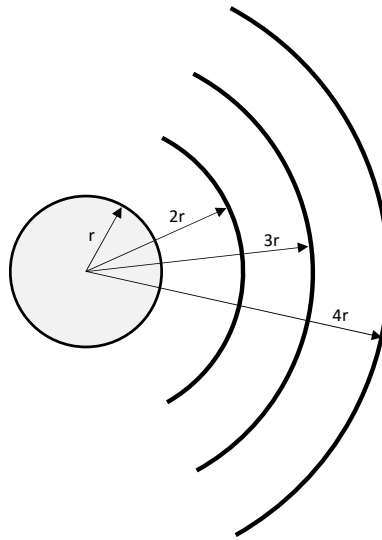


Figure 5. Deflection basis measurement kit positioned at $2r$, $3r$, and $4r$ positions (where ' r ' is the radius of the plate) from the plate center axis.

Eq. (4) as suggested by AASHTO (1993) can be used to determine subgrade layer resilient modulus value:

$$M_{r-SG} = \frac{(1-\nu^2) \cdot P}{\pi \cdot r' \cdot \delta_{r,r'}} \quad (4)$$

where,

M_{r-SG} is in situ subgrade resilient modulus (psi),

$\delta_{r,r'}$ is the resilient deflection (in.) during the unloading portion of the cycle at $r' = 2r$ or $3r$ or $4r$ away from plate center,

ν is the Poisson ratio (assumed as 0.35), and

P is the cyclic load (lbs).

AASHTO (1993) suggests that the r' must be far enough away that it provides a good estimate of the subgrade modulus, independent of the effects of any layers above, but also close enough that it does not result in a too small value. A graphical solution is provided in AASHTO (1993) to estimate the minimum radial distance based on an assumed effective modulus of all layers above the subgrade and the $\delta_{r=0}$ value. Salt (1998) indicated that if the modulus values are plotted against radial distance r , in linear elastic materials such as sands and gravels, the modulus values decrease with increasing distance and then level off after a certain distance. The distance at which the modulus values level off can be used as r' in Eq. 4. In some cases the modulus values decrease and then increase with distance. Such conditions represent either soils with moderate to high moduli with poor drainage at the top of the subgrade or soft soils with low moduli. In those cases the distance where the modulus is low can be used as r' in Eq. 4. In this study, $r' = 2r$ or $3r$ were used to determine M_{r-SG} .

Ullidtz (1987) described Odemark's method of equivalent thickness (MET) concept, as illustrated in Figure 4, which shows a two-layered system on the left part with different moduli values for each layer. M_{r1} represents the resilient modulus of the top layer, M_{r2} represents the resilient modulus of the bottom layer, and h represents the thickness of the top layer. The Odemark's MET concept is that the top layer is transformed into a layer of equivalent thickness h_e with properties of the bottom layer (Ullidtz 1987). The h_e is calculated using Eq. (5), which can be simplified to Eq. (6), if Poisson's ratio (ν) is assumed as the same for the two layers:

$$h_e = h \times \sqrt[3]{\frac{M_{r1}(1-\nu_1^2)}{M_{r2}(1-\nu_2^2)}} \quad (5)$$

$$h_e = h \times \sqrt[3]{\frac{M_{r1}}{M_{r2}}} \quad (6)$$

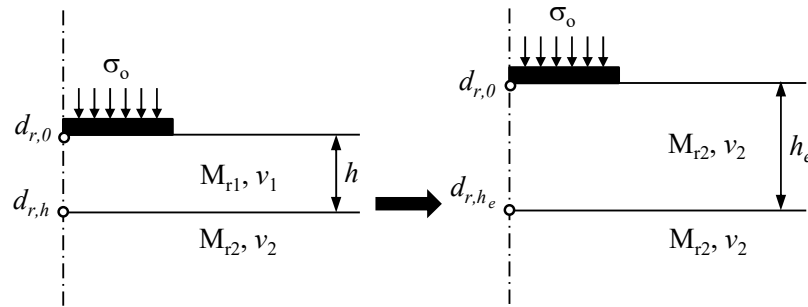


Figure 6. Illustration of Odemark's MET concept.

Using the Boussinesq's solution for linear-elastic materials and Odemark's MET method, Eq. (7) from AASHTO (1993) can be solved to determine the resilient modulus of the base layer (M_{r-Base}):

$$\delta_c = (1 - \nu^2) \sigma_0 r f \left[\frac{1}{M_{r-SG} \sqrt{1 + \left(\frac{h}{r} \times 3 \sqrt{\frac{M_{r-Base}(1 - \nu_1^2)}{M_{r-SG}(1 - \nu_2^2)}} \right)^2}} + \frac{\left(1 - \frac{1}{\sqrt{1 + \left(\frac{h}{r} \right)^2}} \right)}{M_{r-Base}} \right] \quad (7)$$

where,

ν_1 and ν_2 are Poisson ratio's for base and subgrade layer, respectively (assumed as 0.40 and 0.35, respectively), and h is the thickness of the base layer (in.).

Past research has shown that stress measurements in two-layer systems of aggregate base over compressible subgrade are very similar to those predicted by Boussinesq's analysis (e.g., McMahon and Yoder, 1960; Sowers and Vesic, 1961).

The two-layered analysis using the Odemark method is applicable for conditions with moduli values decreasing with depth (i.e., hard over soft), preferably by a factor of at least two between the consecutive layers (Ullidtz 1987). Ullidtz (1987) also noted that the h_e should be larger than the radius of the loading plate, i.e., $h_e/r > 1$.

The M_{r-SG} and M_{r-Base} values were calculated at different applied stress levels from layered analysis to assess the stress-dependent behavior of each layer. Similar to in situ composite M_r values, the calculated M_{r-SG} and M_{r-Base} values were used to model the behavior using the “universal” model (AASHTO 2015) shown in Eq. (3).

In modeling M_{r-Base} behavior, the bulk stress (θ) values are the same as the σ_{cyclic} stress. In case of M_{r-SG} , the θ values were calculated using the following steps:

1. The applied cyclic stress at the base/subgrade interface was calculated using the KENLAYER layered elastic analysis program. The interface stresses are a function M_{r-Base}/M_{r-SG} ratio, thickness of the base layer, radius of the plate, and the applied cyclic stress at the surface (see Huang 2004). The stresses were calculated at the center of the plate.
2. The applied vertical stress (σ_1) is calculated by adding the calculated cyclic stress at the interface and confining stress due to the aggregate layer over the subgrade (0.535 psi).
3. The horizontal stresses (σ_2 and σ_3) were calculated using the procedure described under Section 2.1.1, assuming $\nu = 0.35$ for subgrade.
4. The bulk stress (θ) values were calculated as the sum of σ_1 , σ_2 , and σ_3 .

The analysis approach described above is based on the assumption of a flexible loading plate with uniform stress distribution at the surface and the assumption that both subgrade and base layers are linear elastic with homogenous conditions. The calculated stress values at the interface should therefore be considered approximate.

2.1.3 *Permanent Deformation Monitoring*

Permanent deformation results from cumulative plastic shear strain, compaction, and consolidation during loading. Permanent deformation (δ_p) was monitored during cyclic plate load testing. From the number of load cycles (N) versus δ_p plot, a deformation performance prediction model was developed to analyze and forecast the number of cycles to achieve a selected permanent deformation in the foundation layers. A power model was

selected to represent the permanent deformation versus number of cycles as shown in Eq. 8:

$$\delta_p = CN^d \quad (8)$$

where, coefficient C is the plastic deformation after the first cycle of repeated loading, and d is the scaling exponent.

Monismith et al. (1975) described a similar power model relationship for relating permanent strain to cycle loadings for repeated triaxial laboratory testing. It is expected that C depends on the soil type, soil physical state, and stress conditions (See Li and Selig 1994) and d is expected to be relatively independent of these factors including resilient deflection.

The rate change of the permanent deformation is used herein to estimate the post-compaction permanent deformation and the corresponding number of loading cycles. Post-compaction permanent strain is a function of the shear stress magnitude and can reach an equilibrium state following the “shakedown” concept (see Dawson and Feller, 1999).

A change in permanent deformation rate ($\Delta\delta_p/\text{cycle}$) of 1E-06 in./cycle or less was selected to represent the near-linear elastic condition. The permanent deformation rate is the derivative of the deformation power model function (see Eq. 8). The number of cycles corresponding to $\Delta\delta_p$ of 1E-06 in./cycle is referred to as N^* , where the application of additional cyclic loadings results in very low accumulation of additional permanent deflection and the composite foundation layers are effectively producing a resilient response. δ_p at N^* is the permanent deformation often referred to as the post-compaction deformation. At N^* cycles and the associated permanent deformation, a stable equilibrium response from loading is anticipated (e.g., Collins et al. 1993).

2.2 Dynamic Cone Penetration (DCP) Testing

DCP tests were performed in accordance with ASTM D6951-03 “Standard Test Method for Use of the Dynamic Cone Penetrometer in Shallow Pavement Applications”. The tests involved dropping a 17.6 lb hammer from a height of 22.6 in. and measuring the resulting penetration depth (Fig. 7). A 30 in. penetrating rod was used. California bearing ratio (CBR) values were determined using Eqs. (9) and (10), whichever is appropriate, where the dynamic penetration index (DPI) is in units of mm/blow.

$$CBR(\%) = \frac{292}{DPI^{1.12}} \text{ for all materials except CL soils with CBR } < 10 \quad (9)$$

$$CBR(\%) = 1 / (0.017019 \times DPI)^2 \text{ for CL soils with CBR } < 10 \quad (10)$$

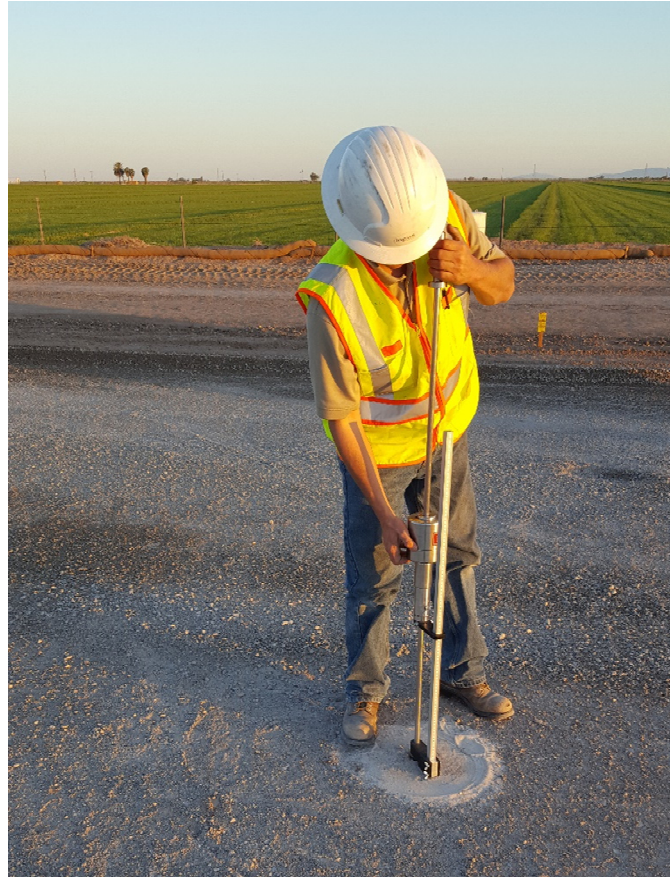


Figure 7. DCP test on aggregate base layer.

2.3 Laboratory Testing

Laboratory tests were performed on bulk samples of aggregate base materials obtained from the test section, to determine the soil gradation parameters and soil classification.

A soil grain-size analysis test was conducted in accordance with ASTM C136M-14 “Standard Test Method for Sieve Analysis of Fine and Coarse Aggregates”. Tests were conducted on oven-dried material. Material was first washed through the No. 200 sieve and the material retained on the No. 200 sieve was oven-dried and dry sieved.

The material was classified in accordance with ASTM D2487-11 “Standard Practice for Classification of Soils for Engineering Purposes (Unified Soil Classification System)” and ASTM D3282-09 “Standard Practice for Classification of Soils and Soil-Aggregate Mixtures for Highway Construction Purposes”.

3 Experimental Study

3.1 Field Experimental Study

For this project, the field testing program involved a series of cyclic plate load tests. Table 2 provides details of the APLT configuration, load cycles, and cyclic stresses used in this study.

Table 2. Summary of plate tests and configurations.

Test Designation	Step	Number of Cycles, N	Cyclic Stress, σ_{cyclic} [psi]	Min. Stress, $\sigma_{min.}$ [psi]	Plate Configuration/ Notes
	Conditioning	500	13.5		
A	1	100	3.5		
	2	100	8.5		
	3	100	13.5	1.5	12 in. diameter flat plate including deflection readings @ 2r and 3r.
	4	100	18.5		
	5	100	28.5		
	6	100	38.5		
B	1	6,000	8.5	1.5	12 in. diameter flat plate
C	1	5,000	18.5	1.5	

The roadway sections in this study contained geogrid between the aggregate base course layer and the underlying subgrade. Table 3 identifies the geogrid used in the field testing program.

Table 3. Summary geogrid material mechanical properties.

Geogrid	Type	Mechanical Properties
TX160	Multi-axial geogrid with hexagonal structure and triangular apertures	Rib pitch longitudinal and diagonal 1.6 inch (40 mm)

The results presented herein represent a selected number of measurements per sample group that was feasible for the site conditions and/or time available for testing. Statistical determination of the minimum number of

measurements requires knowledge of the coefficient of variation within a sample group and the difference between mean values of the selected sample groups. Determination of statistical input parameters needed for calculating statistical sample sizes was beyond the scope of this study.

3.2 Project Details

Table 4 provides details for the project location and nominal profiles of the roadway test areas. Figure 8 shows the May 9-10, 2016 APLT test locations. The locations are based on an average of 2 Hz autonomous GPS measurements at each test location. A *.kmz file that allows greater detail for viewing the test locations is provided separate from this report.

Table 4. Summary of project location and notes.

Site/Location	Notes
Interstate 8, East of City of El Centro between Bonds Corner Road and S33, California; Coordinates: 32°46'23.64"N, 115°19'41.12"W to 32°46'23.39"N, 115°18'15.12"W	Nominal 6 inches of aggregate base course over a subgrade with CBR = < 1 to 40. TX160 placed at the subgrade/base interface. To be paved with CRCP pavement.

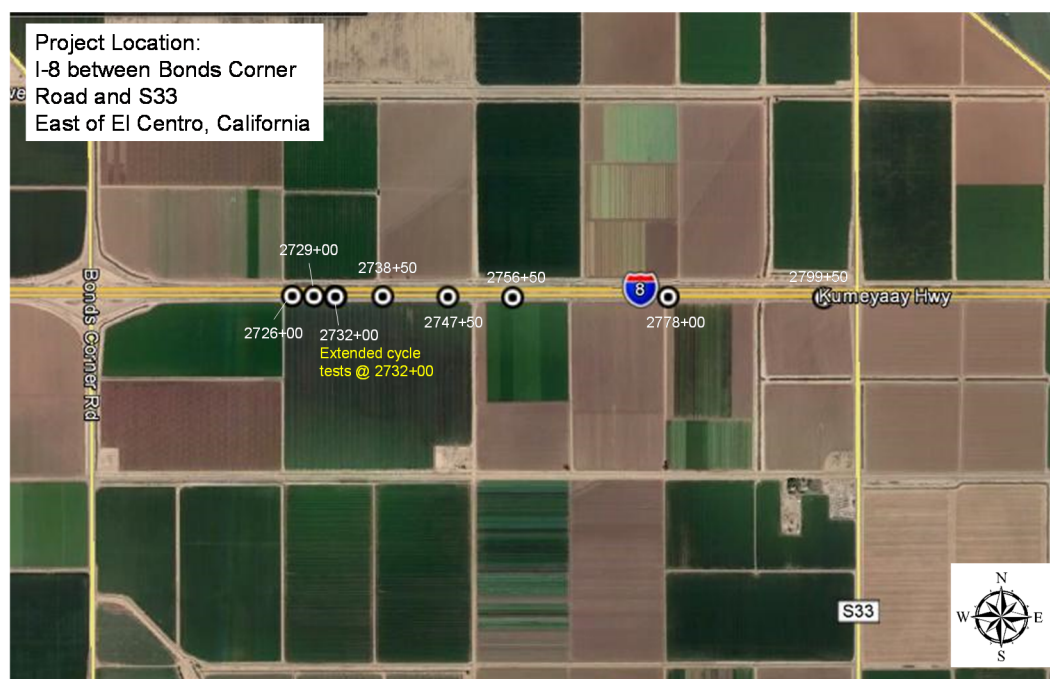


Figure 8. In situ APLT test locations on May 9-10, 2016 on I-8 near El Centro, California.

Figure 9 shows the compacted aggregate base material placed over TX160 geogrid. The APLT test setup is shown in Figure 10.

Figure 11 presents pictures of the loose material used in particle-size analysis and gravel size material (coarser than No. 4 sieve). Figure 12 presents particle-size analysis results of the aggregate base material.



Figure 9. Compacted recycled concrete aggregate (RCA) over TX160 geogrid (May 9, 2016).

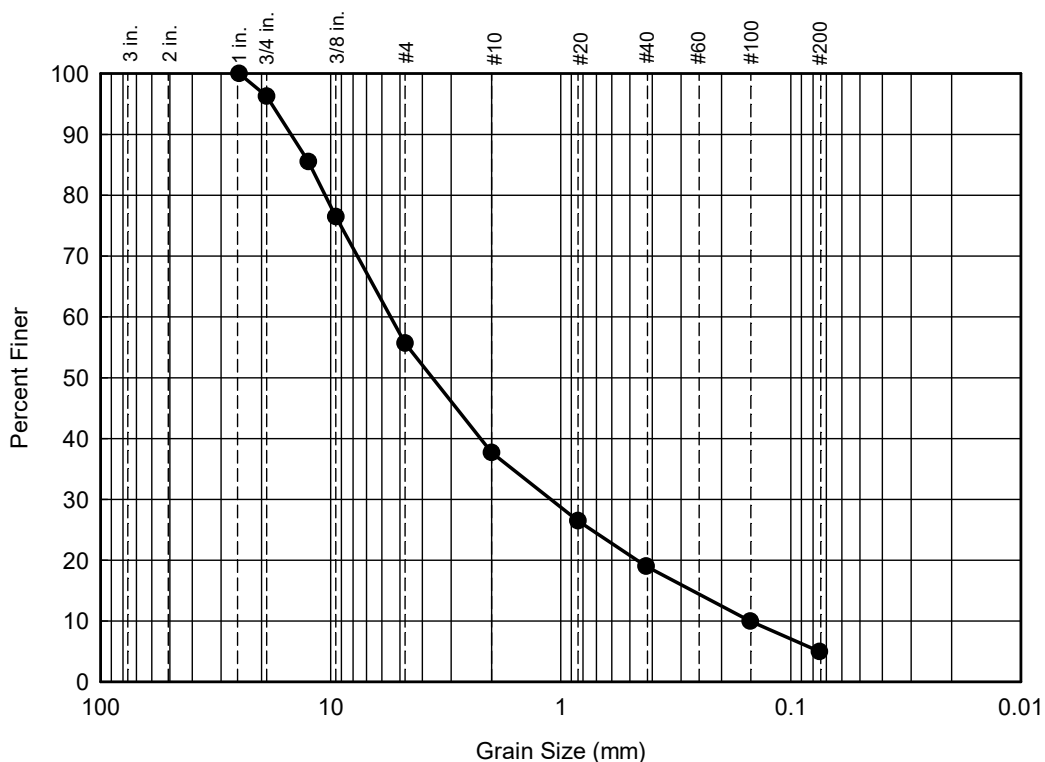


Figure 10. APLT testing at Sta. 2726+00 (May 9, 2016).



Figure 11. (top) Full recycled concrete aggregate (RCA) gradation sample and (bottom) material retained on No. 4 sieve after washing and oven-drying (May 10, 2016 sample).

The material consists of a maximum particle size of 1.0 in. with about 5% passing the No. 200 sieve, and is classified as well-graded sand with silt and gravel (SW-SM) according to the USCS classification and A-1-a according to the AASHTO classification. The material consisted of a mixture of recycled concrete aggregate (RCA).



% Gravel		% Sand			% Fines
Coarse	Fine	Coarse	Medium	Fine	Silt + Clay
3.7	40.6	18.0	18.7	14.0	5.0

Gradation Parameters						
D ₁₀ = 0.152	D ₃₀ = 1.205	D ₅₀ = 3.884	D ₆₀ = 5.741	D ₈₅ = 12.332	c _u = 37.790	c _c = 1.666

Atterberg Limits			Classification	
PL = NP	LL = NP	PI = NP	USCS = SW-SM Well graded sand with gravel and silt	AASHTO = A-1-a

Figure 12. Grain-size analysis and classification of recycled concrete aggregate (RCA) base (sampled May 9, 2016).

4 Results

4.1 Dynamic Cone Penetration (DCP) Test Results

CBR and cumulative blows profiles are included in the Appendix as part of the layered analysis test results summary at each test location. The CBR values for the subgrade were calculated assuming that the subgrade material is classified as lean clay (CL).

The profiles show CBR generally increasing with depth within in the base layer (up to 6 inches below surface) from about 10 to 40. The increasing CBR with depth is typically a result of increasing confinement with depth.

Below the aggregate base layer, the subgrade CBR at all test locations except Sta. 2799+50 decreased with depth up to about 18 inches below the aggregate base layer surface where the lowest CBR values ranged between <1 to 2. The lowest CBR values (about 0.6) were encountered in the subgrade layer at Sta. 2738+50 and 2729+00.

At Sta. 2799+50, the subgrade was reportedly over-excavated and replaced with compacted granular material. At that location, the CBR increased below the base layer from about 50 to over 100 up to 21 inches below surface and then decreased with depth up to the DCP termination depth of about 33 in. below surface.

4.2 In Situ Composite Resilient Modulus

A summary sheet was developed for each test point to document the in situ composite resilient modulus (M_{r-comp}), stress-dependent model parameters k_1^* , k_2^* , and k_3^* (where “*” indicates in situ), break-point resilient modulus ($M_{r-comp(pred.)-BP}$) corresponding to the maximum value over the stress range tested and the associated break-point cyclic stress ($\sigma_{cyclic-BP}$), the permanent deformation (δ_p), and deformation mode (near-linear elastic or plastic) and the associated deformation scaling exponent (d).

The test results provided in the test summaries show that the modulus values are stress sensitive. All tests except one (Sta. 2799+50 where it was reported that the subgrade was overexcavated and replaced with granular material) showed a decrease in M_{r-comp} with increasing cyclic stress. This decrease in modulus is characteristic of composite aggregate base over soft

subgrade, where with stress increasing, the composite modulus decreases as a reflection of the underlying softer subgrade. At Sta. 2799+50, the M_{r-comp} value increased with increasing cyclic stress, which is typically a characteristic of granular material behavior. Based on DCP testing at that test location, the granular layer extended to about 30 in. below the surface.

Table 5 summarizes the in situ M_{r-comp} values for the highest and last stress sequence, which represent the average of the last 5 cycles, and permanent deformation at the end of the test. The M_{r-comp} values ranged between 10.2 ksi and 22.5 ksi at all test locations except at Sta. 2799+50 where the M_{r-comp} was about 39.2 ksi. The average M_{r-comp} was about 16.5 ksi. Tabulated test results for all stress levels are provided in the Appendix.

Table 5. Comparison of in situ M_{r-comp} and permanent deformation results for 12 in. plate APLT tests for the last applied stress sequence ($\sigma_{cyclic} = 38.5$ psi).

Station	In situ M_{r-comp} (psi) (cycles 1095-1100)	δ_p at end of test (in.)
2726+00	22,486	0.068
2729+00	15,930	0.105
2732+00	15,199	0.107
2738+50	18,217	0.083
2747+50	10,238	0.153
2756+50	19,752	0.053
2778+00	13,910	0.044
2799+50*	39,244*	0.015*
Minimum	10,238	0.044
Maximum	22,486	0.153
Average	16,533	0.088

*Test point excluded from average and min./max. summary due to granular subgrade material.

Table 6 summarizes the stress-dependent model parameters k_1^* , k_2^* , and k_3^* , $M_{r-comp (pred.)-BP}$ values, and the associated $\sigma_{cyclic-BP}$. Results show that the break point cyclic stress was about 3.0 psi at all test locations, except at Sta. 2799+50 where the break point stress was at 39 psi. The $M_{r-comp (pred.)-BP}$ ranged between 17.8 ksi and 32.6 ksi.

The k_1^* , k_2^* , and k_3^* model parameters averaged 1,384.9, -0.190, and 0.495, respectively, and are in-line with what would be expected for laboratory determined values. On average, the measured M_{r-comp} versus predicted composite resilient modulus ($M_{r-comp (pred.)}$) showed a standard error of

about 2.7%, suggesting that the model parameters provide a statistically significant and quality fit to the experimental data.

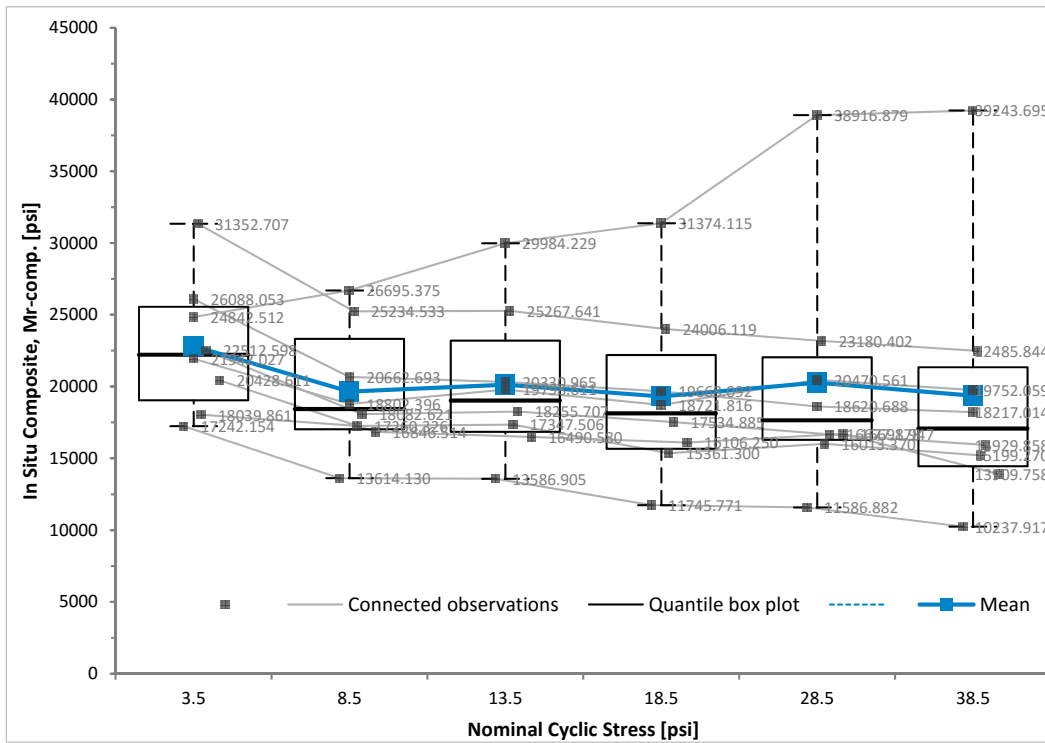
Table 6. Comparison of “universal” model regression parameters for in situ M_{r-comp} , break point cyclic stress, and predicted in situ M_{r-comp} at break point stress.

Station	k_1^*	k_2^*	k_3^*	Adj. R^2	Std. Error (psi)	M_{r-comp} (pred.)-BP [psi]	$\sigma_{cyclic-BP}$ [psi]
2726+00	1,822.0	-0.233	0.748	0.956	646	32,587	3.0
2729+00	1,329.9	-0.208	0.544	0.935	564	23,202	3.0
2732+00	1,211.1	-0.050	-0.185	0.737	536	18,372	3.0
2738+50	1,487.4	-0.258	0.853	0.967	505	27,192	3.0
2747+50	1,040.6	-0.210	0.004	0.954	514	17,873	3.0
2756+50	1,286.3	-0.208	1.299	0.564	629	22,994	3.0
2778+00	1,266.2	-0.166	0.202	0.782	885	21,181	3.0
2799+50*	1,635.4*	0.044*	1.281*	0.938*	1,483*	40,717*	39.0*
Minimum	1,040.6	-0.258	-0.185	0.564	505	17,873	3.0
Maximum	1,822.0	-0.050	1.299	0.967	885	32,587	3.0
Average	1,384.9	-0.190	0.495	0.842	611	23,343	3.0

*Test point excluded from average and min./max. summary due to granular subgrade material.

Figure 13 shows a box plot and descriptive statistics for all test points for the composite resilient modulus results. A trendline for the mean value as a function of the nominal cyclic stress is also provided.

In the individual summary sheets included in the Appendix, the change in permanent deformation ($\Delta\delta_p$) and deformation scaling exponents (d) for each load step are summarized. As expected, permanent deformation increased with increasing cyclic stress. At higher stresses (> 20 psi), most test locations showed that near-linear elastic behavior was not achieved based on modeling each of the 100 cycle load steps. Forecasting of permanent deformation values at higher loading cycles (e.g., 1,000,000 cycles) can only be reliability quantified with extended cycle tests where the number of cycles is extended until the behavior mode reaches near-linear elastic behavior. The results of extended cycle tests are presented in the following sections along with predicted long-term trafficking performance results.



N	8					
	N	Mean	Mean SE	SD		
3.5	8	22806.0654	1626.35893	4600.0377		
8.5	8	19649.8235	1552.80148	4391.9858		
13.5	8	20132.7680	1846.63809	5223.0813		
18.5	8	19314.7935	2130.95908	6027.2625		
28.5	8	20270.6134	2921.94045	8264.4956		
38.5	8	19371.9269	3129.88561	8852.6534		
	Minimum	1st Quartile	Median	3rd Quartile	Maximum	Inter-quartile range
3.5	17242.154	19035.1735	22227.3125	25569.0776	31352.707	6533.9041
8.5	13614.130	17018.9357	18442.5085	23329.5997	26695.375	6310.6640
13.5	13586.905	16847.6325	19027.1590	23210.6927	29984.229	6363.0602
18.5	11745.771	15671.6958	18128.3505	22198.6078	31374.115	6526.9119
28.5	11586.882	16289.9567	17659.8175	22051.3016	38916.879	5761.3449
38.5	10237.917	14447.0547	17073.4360	21346.7669	39243.695	6899.7123

Figure 13. Box plot (top) and descriptive statistics (bottom) for all in situ composite resilient modulus tests for six cyclic stress values.

4.3 Layered Analysis

A summary sheet was developed for each test point to document M_{r-Base} , M_{r-SG} , calculated stresses at the base/subgrade interface, and stress-dependent model parameters k_1^* , k_2^* , and k_3^* for M_{r-Base} and M_{r-SG} , and are included in the Appendix.

Results of layered analysis from the highest and last stress sequence are summarized in Table 7. Tables 8 and 9 summarize the stress-dependent model parameters k_1^* , k_2^* , and k_3^* for M_{r-Base} and M_{r-SG} , respectively. Tabulated test results for all stress levels are provided in the Appendix.

M_{r-Base} values ranged between 40.9 ksi and 65.7 ksi, while the M_{r-SG} values ranged between 4.4 ksi and 12.7 ksi. The M_{r-SG} value at Sta. 2799+50 showed higher M_{r-SG} of 25.6 ksi, as should be expected because of the reported over-excavation and replacement with compacted granular material at that location.

The k_1^* , k_2^* , and k_3^* model parameters averaged 3076, 0.112, and -0.085, respectively for the aggregate base layer and 686, -0.182, and -0.185, respectively for the subgrade layer.

Table 7. Comparison of in situ M_{r-comp} , M_{r-Base} , and M_{r-SG} results for 12 in. plate APLT tests for the last applied stress sequence ($\sigma_{cyclic} = 38.5$ psi).

Station	In situ M_{r-comp} (psi) (cycles 1095-1100)	In situ M_{r-Base} (psi) (cycles 1095-1100)	In situ M_{r-SG} (psi) (cycles 1095-1100)	M_{r-Base}/M_{r-SG} (cycles 950- 1000)
2726+00	22,486	54,938	12,650	4.3
2729+00	15,930	45,379	8,224	5.5
2732+00	15,199	51,326	6,848	7.5
2738+50	18,217	61,914	8,519	7.3
2747+50	10,238	40,946	4,444	9.2
2756+50	19,752	65,771	9,369	7.0
2778+00	13,910	45,081	8,373	5.4
2799+50*	39,244*	72,395*	25,612*	2.8*
Minimum	10,238	40,946	4,444	4.3
Maximum	22,486	65,771	12,650	9.2
Average	16,533	52,194	8,347	6.6

*Test point excluded from average and min./max. summary due to granular subgrade material.

Table 8. Comparison of “universal” model regression parameters for in situ aggregate base layer, M_{r-Base} .

Station	k^*_1	k^*_2	k^*_3	Adj. R^2	Std. Error (psi)
2726+00	3,425.7	0.277	-1.262	0.553	1,495
2729+00	2,677.5	0.669	-3.172	0.851	1,523
2732+00	3,129.4	0.400	-1.875	0.863	2,280
2738+50	4,438.4	-0.321	1.518	0.782	3,802
2747+50	3,969.3	-0.259	0.397	0.891	3,140
2756+50	2,164.2	0.204	1.076	0.939	2,822
2778+00	1,725.4	-0.188	2.722	0.954	1,352
2799+50*	1,883.4*	-0.168*	3.855*	0.888*	5,558*
Minimum	1,725.4	-0.321	-3.172	0.553	1,352
Maximum	4,438.4	0.669	2.722	0.954	3,802
Average	3,075.7	0.112	-0.085	0.833	2,345

*Test point excluded from average and min./max. summary due to granular subgrade material.

Table 9. Comparison of “universal” model regression parameters for in situ subgrade layer, M_{r-SG} .

Station	k^*_1	k^*_2	k^*_3	Adj. R^2	Std. Error (psi)
2726+00	952.4	-0.214	0.377	0.993	169
2729+00	732.8	-0.102	-1.051	0.929	355
2732+00	494.7	-0.296	0.812	0.937	326
2738+50	524.0	-0.323	1.869	0.952	316
2747+50	320.6	-0.307	0.706	0.982	150
2756+50	898.9	-0.001	-1.915	0.973	174
2778+00	877.1	-0.032	-2.090	0.981	195
2799+50	1,724.8	0.264	-0.953	0.981	363
Minimum	320.6	-0.323	-2.090	0.929	150
Maximum	952.4	-0.001	1.869	0.993	355
Average	685.8	-0.182	-0.185	0.964	241

*Test point excluded from average and min./max. summary due to granular subgrade material.

The M_{r-Base} values at six out of the eight test locations generally showed increasing modulus with increased cyclic stress, which is a characteristic of granular material. However, at four of those six locations, there was a decrease in modulus from load step 1 to 2. The first load step was not

included in determining the regression parameters for those tests. At two test locations, the M_{r-Base} values showed decreasing modulus with decreasing cyclic stress.

The M_{r-SG} values decreased with increasing cyclic stress at all locations except at Sta. 2799+50, which is a characteristic of cohesive subgrade material. At Sta. 2799+50, where the M_{r-SG} values increased with increasing cyclic stress, which is a characteristic of granular material.

4.4 Forecasting Trafficking Performance

A summary sheet was prepared for each of the two tests showing the permanent deformation model parameters (C and d), the number of cycles (N^*) to achieve near-linear elastic δ_p rate limit ($\Delta\delta_p = 1E-06$ in./cycle), δ_p at N^* , and number of cycles (N) to achieve a $\delta_p = 0.05$ to 0.1 in., and is included in the Appendix.

Table 10 summarizes C and d parameters for the two tests with comparisons between N^* , δ_p at N^* , and adjusted δ_p at N^* , and N to reach $\delta_p = 0.05$ in.

The N^* value ranged from 2.1 to 2.2 k cycles for the two tests. The N value to reach $\delta_p = 0.05$ in. at $\sigma_{cyclic} = 8.5$ psi is about 4.7 million cycles while at $\sigma_{cyclic} = 18.2$ psi it is about 84k cycles.

Table 10. Summary of permanent deformation prediction parameters.

Station	Cyclic Stress (psi)	C	d	R^2	N^* at $\Delta\delta_p = 1E-06$ in./cycle	δ_p (in.) at N^*	Adj. δ_p (in.) at N^*	N at $\delta_p = 0.05$ in.
2732+00*	8.5	0.0137	0.0842	0.9790	2,209	0.026	0.013	4,688,705
2732+00*	18.2	0.0284	0.0499	0.9764	2,073	0.042	0.013	83,546

* Note: Test points adjacent to Sta. location, but not at exact same point (~3 ft separation)

5 Summary

A summary of the key observations from the tests conducted in this study are as follows:

1. The road section selected for in situ performance assessment provided an excellent opportunity to evaluate recycled concrete aggregate (RCA) base stabilized with TX160 geogrid. The aggregate base course classified as well-graded sand with silt and gravel (SW-SM) with 5.0% fines content.
2. DCP-CBR profiles generally increased with depth within in the aggregate base layer (up to 6 inches below surface) from about 10 to 40. Below the base layer, the CBR at all test locations except one (Sta. 2799+50) decreased with depth at about 18 inches below surface where the lowest CBR values ranged between <1 to 2. At Sta. 2799+50, the subgrade was reportedly over-excavated and replaced with compacted granular material. At this location, the CBR increased from about 50 to over 100 up to 21 inches below surface and then decreased with depth.
3. The in situ M_{r-comp} values are stress sensitive. Most tests exhibited a general decrease in modulus within increasing cyclic stress. This decrease in modulus is a characteristic of composite behavior with aggregate base over softer cohesive subgrade soils.
4. Box plot and descriptive statistics for all in situ M_{r-comp} values provide an assessment of the variability and trend in composite modulus with increasing cycle stress.
5. Using the "universal" model (AASHTO 2015), the k_1^* , k_2^* , and k_3^* model parameters averaged 1,384.9, -0.190, and 0.495, respectively, and are in-line with what would be expected for laboratory determined values. On average, the measured M_{r-comp} versus predicted composite resilient modulus (M_{r-comp} (pred.)) showed a standard error of about 2.7%, suggesting that the model parameters provide a statistically significant and quality fit to the experimental data.
6. Layered elastic analysis accounting for stress at the subgrade layer shows that M_{r-Base} values ranged between 40.9 ksi and 65.8 ksi, while the M_{r-SG} values ranged between 4.4 ksi and 12.7 ksi. k_1^* , k_2^* , and k_3^* model parameters averaged 3,075.7, 0.112, and -0.085, respectively for the aggregate base layer and 685.8, -0.182, and -0.185, respectively for the subgrade layer. Both sets of model parameter values are in-line with expected values and both models are statistically significant.

7. The M_{r-Base} values at six out of the eight test locations generally showed increasing modulus with increased cyclic stress, which is a characteristic of granular material. The M_{r-SG} values decreased with increasing cyclic stress at seven of eight locations, which is a characteristic of cohesive materials.
8. Analysis of permanent deformation (δ_p) and deformation scaling exponents (d) for each load step shows that the permanent deformation increased with increasing cyclic stress, as expected. Modeling permanent deformation response of each load step showed that at cyclic stresses less than about <20 psi, most test locations exhibited a near-linear elastic behavior during loading.
9. Two extended cycle APLT tests (5000 cycles) were performed at two different cyclic stresses (8.5 psi and 18.2 psi) on the aggregate base layer to determine the composite permanent deformation model parameters (C and d), the number of cycles (N^*) to achieve near-linear elastic δ_p rate limit ($\Delta\delta_p = 1E-06$ in./cycle), δ_p at N^* , and number of cycles (N) to achieve a $\delta_p = 0.05$ to 0.1 in. Results demonstrate that N^* ranged from 2.1k to 2.2k cycles for the two tests. The N value to reach $\delta_p = 0.05$ in. at $\sigma_{cyclic} = 8.5$ psi is estimated at 4.7 million cycles while at $\sigma_{cyclic} = 18.2$ psi it is about 84k cycles.

References

- AASHTO T307-99 (2000). "Standard Method of Test for Determining the Resilient Modulus of Soils and Aggregate Materials", Standard Specifications for Transportation Materials and Methods of Sampling and Testing, Twentieth Edition, American Association of State Highway and Transportation Officials, Washington, DC.
- AASHTO T222-81 (2012). "Standard Method of Test for Nonrepetitive Static Plate Load Test of Soils and Flexible Pavement Components for Use in Evaluation and Design of Airport and Highway Pavements", Standard Specifications for Transportation Materials and Methods of Sampling and Testing, Thirty Second Edition, American Association of State Highway and Transportation Officials, Washington, DC.
- AASHTO (1993). *AASHTO Guide for Design of Pavement Structures*, Published by the American Association of State Highway and Transportation Officials, Washington, D.C.
- Brown, S., and Hyde, A. (1975). "Significance of cyclic confining stress in repeated-load triaxial testing of granular material." *Transportation Research Record*, (537).
- Collins, I.F., Wang, A. P. and Saunders, L.R. (1993). Shakedown theory and the design of unbound pavements. *Road and Transport Research*, Vol. 2, No. 4, Dec. pp. 28-39.
- DIN 18134. (2001). "Determining the deformation and strength characteristics of soil by the plate loading test," Technical Committee 05.03.00 Baugrund, Versuche und Versuchsgeräte of the Normenausschuss Bauwesen (Building and Civil Engineering Standards Committee).
- Houston, S. L., Perez-Garcia, N., and Houston, W., N. (2008). "Shear strength and shear-induced volume change behavior of unsaturated soils from triaxial test program." *Journal of Geotechnical and Geoenvironmental Engineering*, Vol. 134, No. 11, p. 1619-1632.
- Huang, Y. H. (2004). *Pavement analysis and design*, Second Edition, Pearson Education, Inc., Upper Saddle River, NJ.

- LeKarp, F., Isacsson, U., and Dawson, A. (2000). "State of the art. I: Resilient response of unbound aggregates." *Journal of Transportation Engineering*, American Society of Civil Engineers.
- Li, D., and Selig, E. T., (1994). Resilient modulus for fine-grained subgrade soils." *Journal of Geotechnical Engineering*, ASCE, 120(6), 939-957.
- McMahon, T. F., and E.J. Yoder, (1960). "Design of a pressure sensitive cell and model studies of pressures on a flexible pavement subgrade." Proceedings, *Highway Research Board*, Vol. 39, pp. 650-682.
- Monismith, C.L., Ogawa, N., and Freeme, C. R. (1975). "Permanent deformation characteristics of subgrade soils due to repeated loading." *Transportation Research Record*, 537, 1-17.
- NCHRP. (2004). "Laboratory Determination of Resilient Modulus for Flexible Pavement Design," Research Results Digest Number 285, National Cooperative Highway Research Program, Transportation Research Board, Washington, D.C.
- Salt G. (1998). "Pavement Deflection Measurement and Interpretation for the Design of Rehabilitation Treatments", *Transfund New Zealand Research Report No. 117*, Wellington, New Zealand.
- Sowers, G. F., and A. B. Vesic. (1961). "Stress distribution beneath pavements of different rigidities." Proceedings, *International Conference on Soils Mechanics and Foundation Engineering*, 5th, vol. 2, pp. 327-332.
- Ullidtz, P. (1987). *Pavement Analysis*, Elsevier, New York, NY.
- Werkmeister, S., Dawson, A., and Wellner, F. (2013). "Permanent deformation behavior of granular materials and the shakedown concept." *Transportation Research Record*, No. 1757, *Journal of the Transportation Research Board*, p. 75-81.
- White, D. J. (2015). "Field Evaluation of Plate Size Corrections for Cyclic Plate Load Testing: Geogrid Stabilized Aggregate Base over Soft Subgrade," *Interim Report*, Ingios Geotechnics, Inc., Boone, Iowa, USA.
- White, D.J., Vennapusa, P., FitzPatrick, B., Cackler, E. T. (2015). "Automated Plate Load Testing Report: I-294 NB and SB Lanes, MP. 17.5 to 29.5, 95th Street to Cermak

Rd. (22nd St.)” *Internal Report No. 2015-024*, Ingios Geotechnics, Inc., Boone, Iowa, USA.

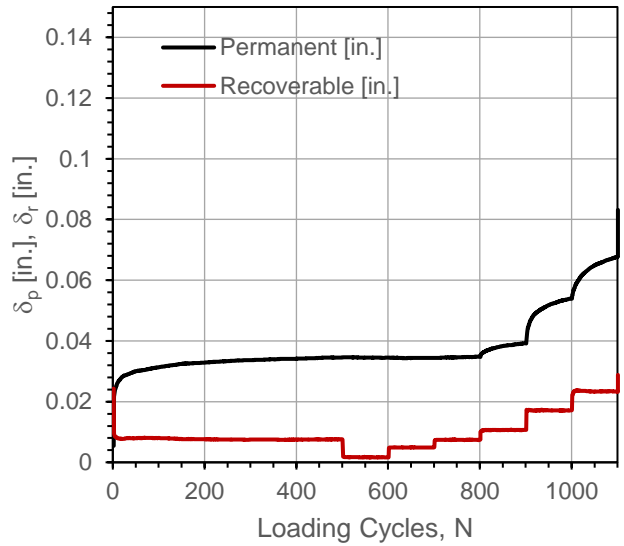
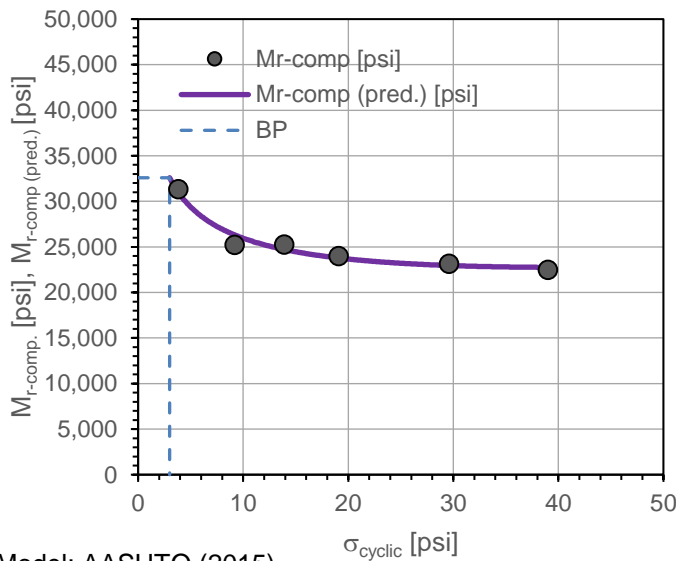
White, D.J. (2016). “In Situ Performance Verification of Geogrid-Stabilized Aggregate Layer: Brown Field Municipal Airport, San Diego, CA.” *DRAFT Report No. 2016-027*, Ingios Geotechnics, Inc., Boone, Iowa, USA.

Appendix: APLT and DCP Test Results and Analysis

Automated Plate Load Test [APLT]

Test:	In-situ Resilient Modulus [Mr]: Cyclic Loading, Composite, Stress-Dependent (5, 10, 15, 20, 30, 40)				
Date:	5/9/2016	Time:	6:39:30 PM	Test ID	I-8_sta2726
Tested By	DW, HG	Location:	East Bound- Center	Sta.	2726
Latitude,N:	32.773232	Longitude,W:	115.328090	Elev. (m):	1.26
Comments:	Recycled aggregate base (0.55 ft) stabilized with TX160 geogrid. Plate size correction ($F_{corrected}$) = 1.00.				

Step	N	σ_{cyclic} [psi]	M_{r-comp} [psi]	$M_{r-comp (pred.)}$ [psi]	δ_p [in.]	$\Delta\delta_p$ [in.]	$d = \Delta\log(\delta_p) / \Delta\log(N)$	Near-linear Elastic
Conditioning	500	13.92	---	---	0.0346	---	0.093	---
1	100	3.83	31,353	30,977	0.0345	-0.0001	-0.212	Y
2	100	9.20	25,235	26,310	0.0344	-0.0002	-0.123	Y
3	100	13.92	25,268	24,711	0.0348	0.0001	0.395	Y
4	100	19.08	24,006	23,783	0.0392	0.0046	0.506	Y
5	100	29.62	23,180	22,957	0.0539	0.0193	0.522	N
6	100	39.03	22,486	22,749	0.0678	0.0331	0.615	N



Model: AASHTO (2015)

$$M_{r-comp} = k_1^* P_a \left(\frac{\theta}{P_a}\right)^{k_2^*} \left(1 + \frac{\tau_{oct}}{P_a}\right)^{k_3^*}$$

Parameter	Value	P-Value
k_1^*	1,822.0	1.86E-07
k_2^*	-0.233	2.42E-02
k_3^*	0.748	1.60E-01
Adj. R^2	0.956	
Std. Error [psi]	646	

$M_{r-comp (pred.)-BP}$ [psi]	32,587
$\sigma_{cyclic-BP}$ [psi]	3.0

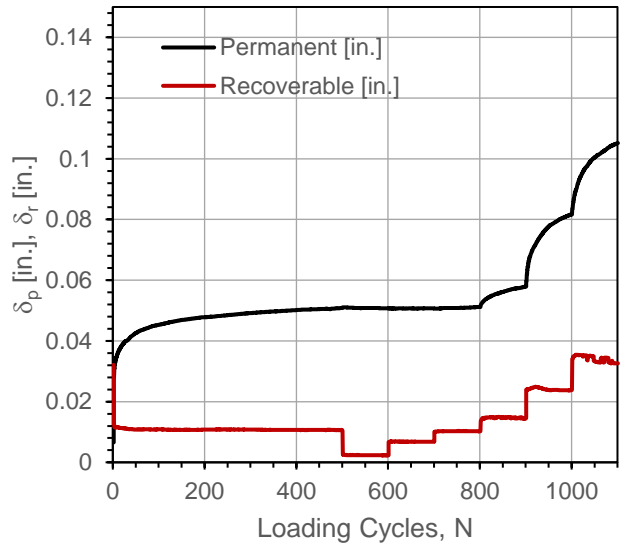
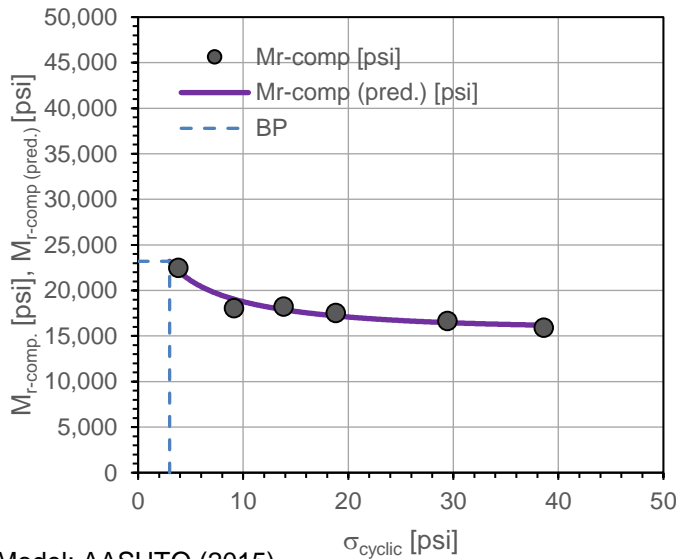


In-situ Resilient Modulus [Mr]: Cyclic Loading, Composite, Stress-Dependent		
Project Name:	I8 El Centro, CA	
Project ID:	Tensar	
Location:	Interstate 8, East Bound, East of Bonds Corner Rd.	

Automated Plate Load Test [APLT]

Test:	In-situ Resilient Modulus [Mr]: Cyclic Loading, Composite, Stress-Dependent (5, 10, 15, 20, 30, 40)				
Date:	5/9/2016	Time:	7:16:18 PM	Test ID:	I-8_sta2729
Tested By:	DW, HG	Location:	East Bound- Center	Sta.:	2729
Latitude, N:	32.773228	Longitude, W:	115.327120	Elev. (m):	1.54
Comments:	Recycled aggregate base (0.55 ft) stabilized with TX160 geogrid. Plate size correction ($F_{corrected}$) = 1.00.				

Step	N	σ_{cyclic} [psi]	M_{r-comp} [psi]	M_{r-comp} (pred.) [psi]	δ_p [in.]	$\Delta\delta_p$ [in.]	$d = \Delta\log(\delta_p) / \Delta\log(N)$	Near-linear Elastic
Conditioning	500	13.87	---	---	0.0510	---	0.104	---
1	100	3.83	22,513	22,162	0.0506	-0.0004	-0.348	Y
2	100	9.14	18,083	19,036	0.0506	-0.0004	0.054	Y
3	100	13.87	18,256	17,890	0.0511	0.0001	0.421	Y
4	100	18.81	17,535	17,208	0.0579	0.0069	0.589	N
5	100	29.44	16,677	16,468	0.0816	0.0306	0.587	N
6	100	38.63	15,930	16,187	0.1051	0.0541	0.647	N



Model: AASHTO (2015)

$$M_{r-comp} = k_1^* P_a \left(\frac{\theta}{P_a}\right)^{k_2^*} \left(1 + \frac{\tau_{oct}}{P_a}\right)^{k_3^*}$$

Parameter	Value	P-Value
k_1^*	1,329.9	4.00E-07
k_2^*	-0.208	5.48E-02
k_3^*	0.544	3.55E-01
Adj. R^2	0.935	
Std. Error [psi]	564	

M_{r-comp} (pred.)-BP [psi]	23,202
$\sigma_{cyclic-BP}$ [psi]	3.0

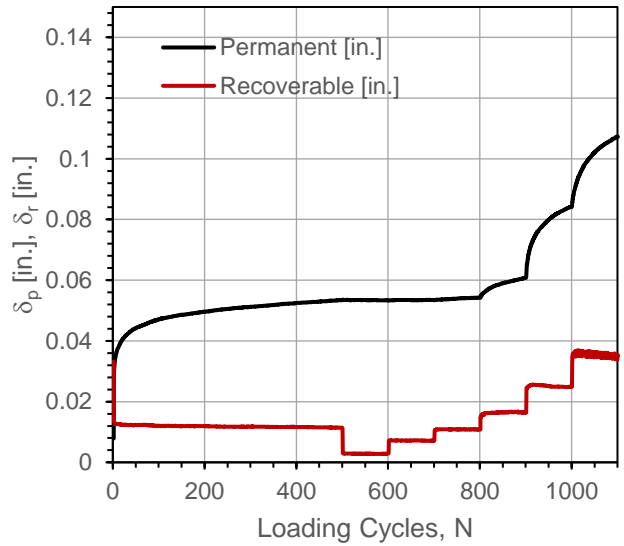
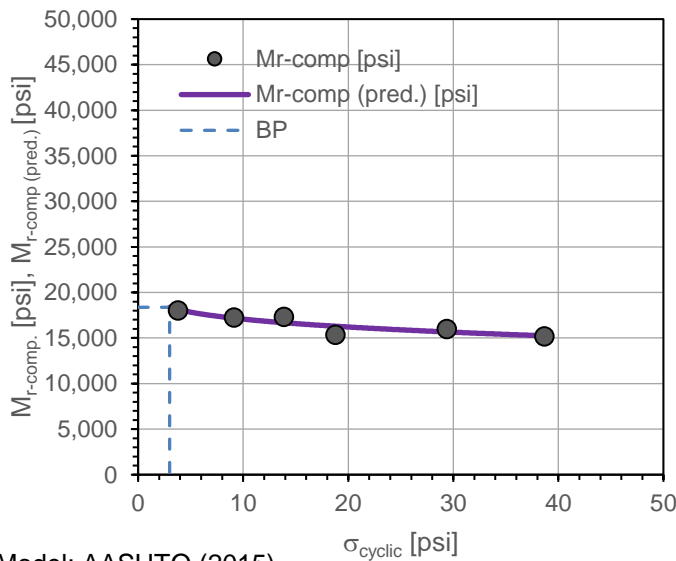


In-situ Resilient Modulus [Mr]: Cyclic Loading, Composite, Stress-Dependent		
Project Name:	I8 El Centro, CA	
Project ID:	Tensar	
Location:	Interstate 8, East Bound, East of Bonds Corner Rd.	

Automated Plate Load Test [APLT]

Test:	In-situ Resilient Modulus [Mr]: Cyclic Loading, Composite, Stress-Dependent (5, 10, 15, 20, 30, 40)				
Date:	5/9/2016	Time:	7:54:11 PM	Test ID	I-8_sta2732
Tested By	DW, HG	Location:	East Bound- Center	Sta.	2732
Latitude,N:	32.773216	Longitude,W:	115.326140	Elev. (m):	0.04
Comments:	Recycled aggregate base (0.55 ft) stabilized with TX160 geogrid. Plate size correction ($F_{corrected}$) = 1.00.				

Step	N	σ_{cyclic} [psi]	M_{r-comp} [psi]	M_{r-comp} (pred.) [psi]	δ_p [in.]	$\Delta\delta_p$ [in.]	$d = \Delta\log(\delta_p) / \Delta\log(N)$	Near-linear Elastic
Conditioning	500	13.88	---	---	0.0536	---	0.111	---
1	100	3.80	18,040	18,128	0.0532	-0.0003	-0.185	Y
2	100	9.15	17,260	17,173	0.0534	-0.0002	0.132	Y
3	100	13.88	17,348	16,678	0.0542	0.0006	0.468	Y
4	100	18.80	15,361	16,290	0.0608	0.0072	0.615	N
5	100	29.40	16,013	15,665	0.0842	0.0306	0.583	N
6	100	38.69	15,199	15,243	0.1073	0.0537	0.663	N



Model: AASHTO (2015)

$$M_{r-comp} = k_1^* P_a \left(\frac{\theta}{P_a}\right)^{k_2^*} \left(1 + \frac{\tau_{oct}}{P_a}\right)^{k_3^*}$$

Parameter	Value	P-Value
k_1^*	1,211.1	6.58E-07
k_2^*	-0.050	5.67E-01
k_3^*	-0.185	7.70E-01
Adj. R^2	0.737	
Std. Error [psi]	536	

M_{r-comp} (pred.)-BP [psi]	18,372
$\sigma_{cyclic-BP}$ [psi]	3.0



In-situ Resilient Modulus [Mr]: Cyclic Loading, Composite, Stress-Dependent

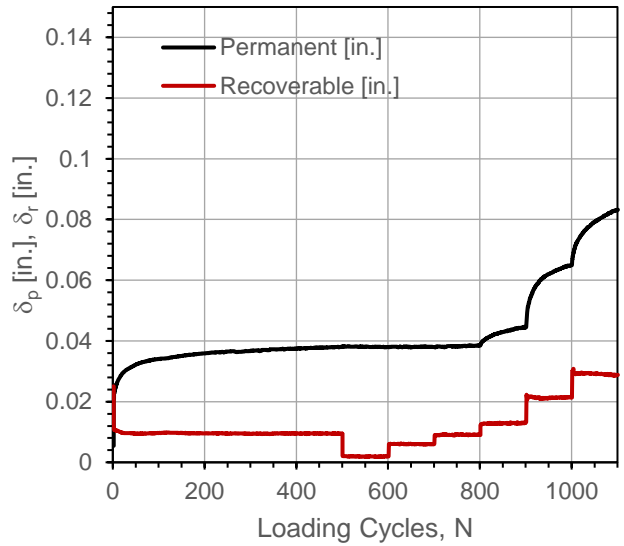
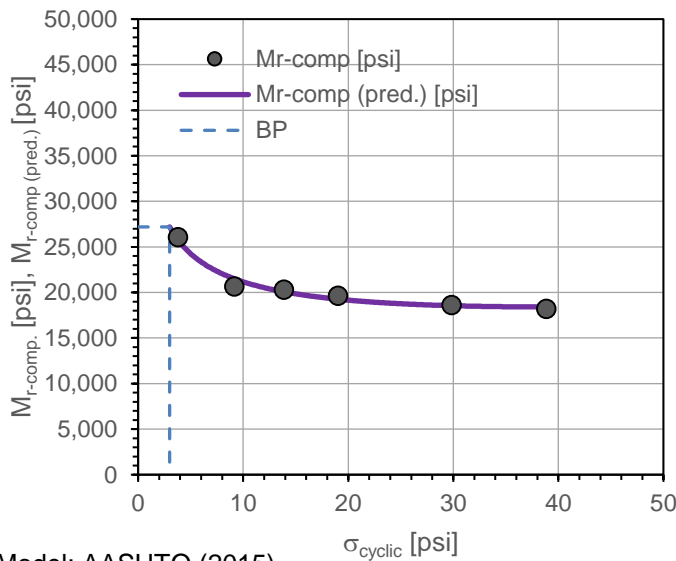
Project Name: I8 El Centro, CA
 Project ID: Tensar
 Location: Interstate 8, East Bound, East of Bonds Corner Rd.



Automated Plate Load Test [APLT]

Test:	In-situ Resilient Modulus [Mr]: Cyclic Loading, Composite, Stress-Dependent (5, 10, 15, 20, 30, 40)				
Date:	5/9/2016	Time:	8:29:43 PM	Test ID	I-8_sta2738_50
Tested By	DW, HG	Location:	East Bound- Center	Sta.	2738_50
Latitude,N:	32.773216	Longitude,W:	115.324020	Elev. (m):	3.61
Comments:	Recycled aggregate base (0.55 ft) stabilized with TX160 geogrid. Plate size correction ($F_{corrected}$) = 1.00.				

Step	N	σ_{cyclic} [psi]	M_{r-comp} [psi]	M_{r-comp} (pred.) [psi]	δ_p [in.]	$\Delta\delta_p$ [in.]	$d = \Delta\log(\delta_p) / \Delta\log(N)$	Near-linear Elastic
Conditioning	500	13.88	---	---	0.0381	---	0.108	---
1	100	3.80	26,088	25,773	0.0379	-0.0002	-0.135	Y
2	100	9.16	20,663	21,501	0.0379	-0.0002	0.069	Y
3	100	13.88	20,331	20,073	0.0385	0.0004	0.330	Y
4	100	19.05	19,668	19,258	0.0445	0.0063	0.597	N
5	100	29.84	18,621	18,548	0.0650	0.0269	0.551	N
6	100	38.87	18,217	18,403	0.0832	0.0450	0.597	N



Model: AASHTO (2015)

$$M_{r-comp} = k_1^* P_a \left(\frac{\theta}{P_a}\right)^{k_2^*} \left(1 + \frac{\tau_{oct}}{P_a}\right)^{k_3^*}$$

Parameter	Value	P-Value
k_1^*	1,487.4	1.77E-07
k_2^*	-0.258	1.59E-02
k_3^*	0.853	1.12E-01
Adj. R^2	0.967	
Std. Error [psi]	505	

M_{r-comp} (pred.)-BP [psi]	27,192
$\sigma_{cyclic-BP}$ [psi]	3.0

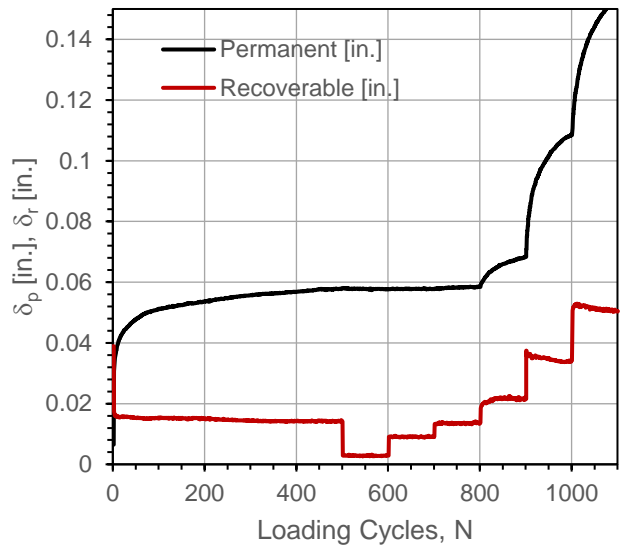
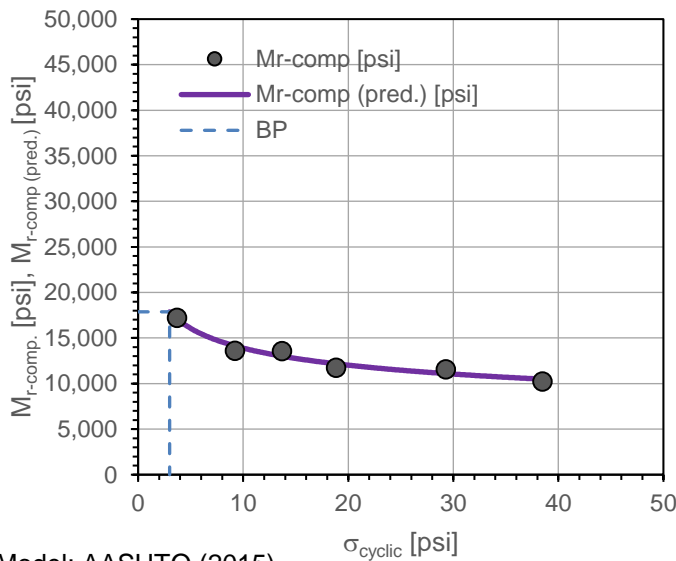


In-situ Resilient Modulus [Mr]: Cyclic Loading, Composite, Stress-Dependent		
Project Name:	I8 El Centro, CA	
Project ID:	Tensar	
Location:	Interstate 8, East Bound, East of Bonds Corner Rd.	

Automated Plate Load Test [APLT]

Test:	In-situ Resilient Modulus [Mr]: Cyclic Loading, Composite, Stress-Dependent (5, 10, 15, 20, 30, 40)				
Date:	5/9/2016	Time:	9:07:28 PM	Test ID	I-8_sta2747_50
Tested By	DW, HG	Location:	East Bound- Center	Sta.	2747_50
Latitude,N:	32.773201	Longitude,W:	115.321090	Elev. (m):	1.75
Comments:	Recycled aggregate base (0.55 ft) stabilized with TX160 geogrid. Plate size correction ($F_{corrected}$) = 1.00.				

Step	N	σ_{cyclic} [psi]	M_{r-comp} [psi]	M_{r-comp} (pred.) [psi]	δ_p [in.]	$\Delta\delta_p$ [in.]	$d = \Delta\log(\delta_p) / \Delta\log(N)$	Near-linear Elastic
Conditioning	500	13.70	---	---	0.0581	---	0.120	---
1	100	3.72	17,242	17,085	0.0577	-0.0004	-0.156	Y
2	100	9.22	13,614	14,130	0.0577	-0.0004	0.098	Y
3	100	13.70	13,587	13,007	0.0585	0.0004	0.421	Y
4	100	18.84	11,746	12,168	0.0684	0.0103	0.671	N
5	100	29.30	11,587	11,096	0.1084	0.0504	0.631	N
6	100	38.50	10,238	10,482	0.1534	0.0954	0.747	N



Model: AASHTO (2015)

$$M_{r-comp} = k_1^* P_a \left(\frac{\theta}{P_a}\right)^{k_2^*} \left(1 + \frac{\tau_{oct}}{P_a}\right)^{k_3^*}$$

Parameter	Value	P-Value
k_1^*	1,040.6	1.02E-06
k_2^*	-0.210	9.55E-02
k_3^*	0.004	9.95E-01
Adj. R^2	0.954	
Std. Error [psi]	514	

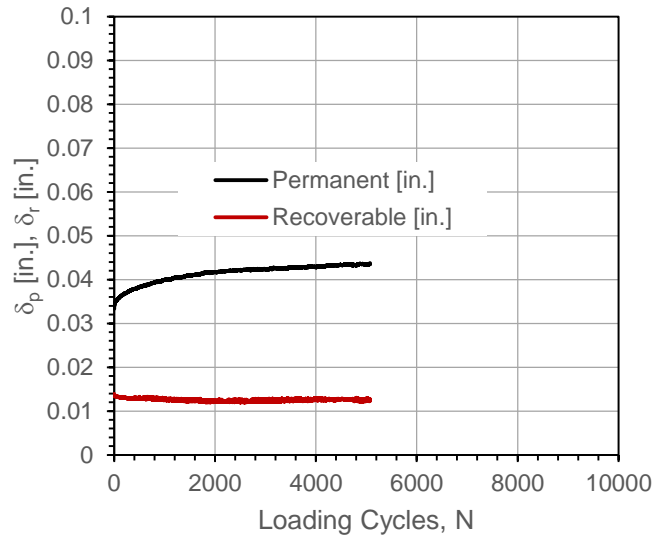
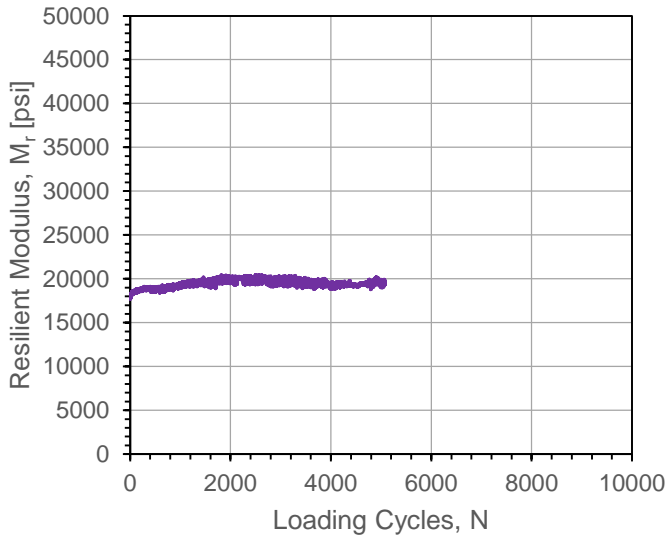
M_{r-comp} (pred.)-BP [psi]	17,873
$\sigma_{cyclic-BP}$ [psi]	3.0



In-situ Resilient Modulus [Mr]: Cyclic Loading, Composite, Stress-Dependent		
Project Name:	I8 El Centro, CA	
Project ID:	Tensar	
Location:	Interstate 8, East Bound, East of Bonds Corner Rd.	

Automated Plate Load Test [APLT]

Test:	In-situ Resilient Modulus [Mr]: Cyclic Loading, 5,000 cycles, Composite [Cyclic Stress = 20 psi]				
Date:	5/10/2016	Time:	12:53:07 PM	Test ID	I8_Extended_20psi
Tested By	DW, HG	Location:	East Bound- Center	Sta.	2732+00
Latitude:	32.773205	Longitude:	115.326147	Elev. (m):	0.6
Comments:	Recycled aggregate base (0.55 ft) stabilized with TX160 geogrid. Plate size correction ($F_{corrected}$) = 1.00.				



$M_{r-comp} =$ 0.19394 psi [Average of the last 10 cycles]
 $\sigma_{cyclic} =$ 0.182 psi

Permanent Deformation Prediction Parameters

$C =$ 0.0284

$d =$ 0.0499

$R^2 =$ 0.9764

$N^* =$ 2,073 Cycles

$\delta_p \text{ at } N^* =$ 0.0416 in.

Adj. $\delta_p \text{ at } N^* =$ 0.0132 in.

$N_{0.05} =$ 83,546 Cycles

$N_{0.1} =$ >>10,000,000 Cycles

$N_{0.15} =$ >>10,000,000 Cycles

$N_{0.20} =$ >>10,000,000 Cycles

$N_{0.25} =$ >>10,000,000 Cycles

$N_{0.30} =$ >>10,000,000 Cycles

$N_{0.40} =$ >>10,000,000 Cycles

$N_{0.50} =$ >>10,000,000 Cycles

Model: $\delta_p = CN^d$

δ_p = permanent deformation

C = plastic deformation after first cycle

d = scaling component

N = Number of loading cycles

N^* = Number of loading cycles at $\Delta\delta_p = 1E-06$ in./cycles

Adj. $\delta_p \text{ at } N^* = \delta_p \text{ at } N^* - C$

N_x = Number of loading cycles to achieve δ_p of x in.

In-situ Resilient Modulus [Mr] and Permanent Deformation [delta_p]: Cyclic Loading

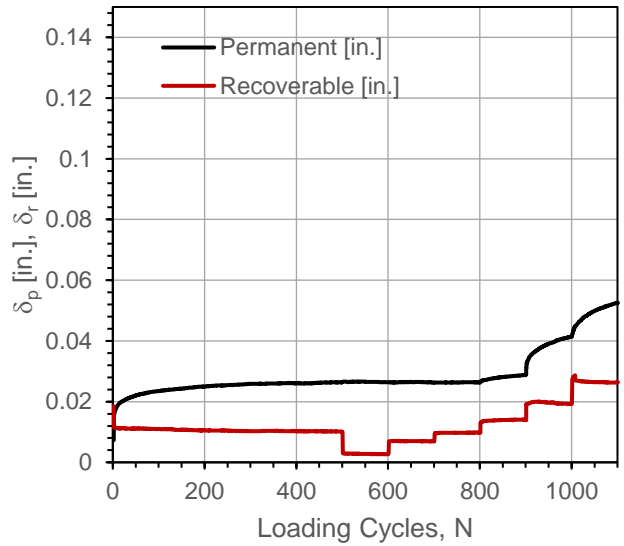
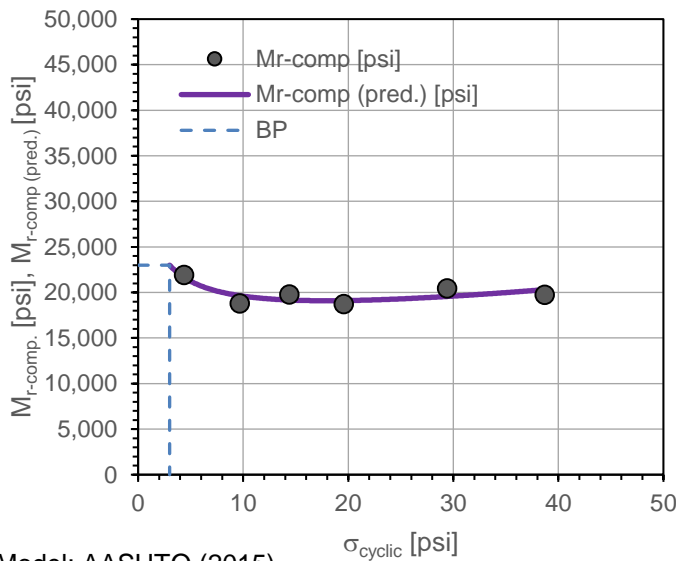
Project Name: I8 El Centro, CA
 Project ID: Tensar
 Location: Interstate 8, East Bound, East of Bonds Corner Rd.



Automated Plate Load Test [APLT]

Test:	In-situ Resilient Modulus [Mr]: Cyclic Loading, Composite, Stress-Dependent (5, 10, 15, 20, 30, 40)				
Date:	5/10/2016	Time:	11:30:55 AM	Test ID	18 2756 50
Tested By	DW, HG	Location:	East Bound- Center	Sta.	2756_50
Latitude,N:	32.773178	Longitude,W:	115.318180	Elev. (m):	8.20
Comments:	Recycled aggregate base (0.55 ft) stabilized with TX160 geogrid. Plate size correction ($F_{corrected}$) = 1.00.				

Step	N	σ_{cyclic} [psi]	M_{r-comp} [psi]	$M_{r-comp (pred.)}$ [psi]	δ_p [in.]	$\Delta\delta_p$ [in.]	$d = \Delta\log(\delta_p) / \Delta\log(N)$	Near-linear Elastic
Conditioning	500	14.40	---	---	0.0265	---	0.101	---
1	100	4.39	21,942	21,639	0.0264	-0.0002	-0.164	Y
2	100	9.68	18,802	19,647	0.0262	-0.0003	0.107	Y
3	100	14.40	19,799	19,167	0.0263	-0.0002	0.143	Y
4	100	19.58	18,722	19,107	0.0289	0.0024	0.486	Y
5	100	29.42	20,471	19,560	0.0413	0.0148	0.460	Y
6	100	38.70	19,752	20,303	0.0526	0.0260	0.607	N



Model: AASHTO (2015)

$$M_{r-comp} = k_1^* P_a \left(\frac{\theta}{P_a}\right)^{k_2^*} \left(1 + \frac{\tau_{oct}}{P_a}\right)^{k_3^*}$$

Parameter	Value	P-Value
k_1^*	1,286.3	8.04E-07
k_2^*	-0.208	1.19E-01
k_3^*	1.299	1.52E-01
Adj. R^2	0.564	
Std. Error [psi]	629	

$M_{r-comp (pred.)-BP}$ [psi]	22,994
$\sigma_{cyclic-BP}$ [psi]	3.0

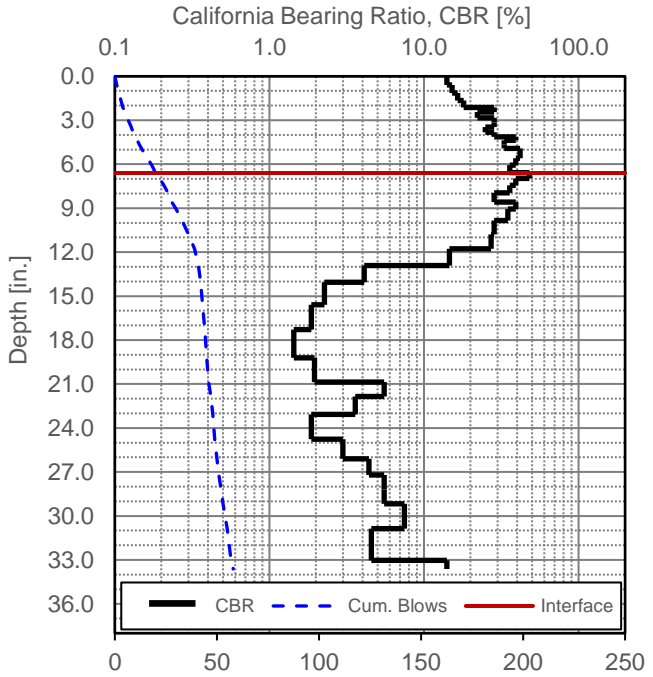
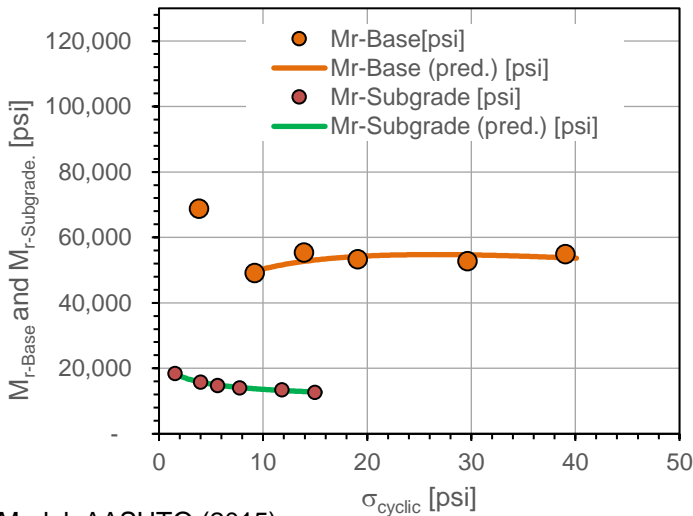


In-situ Resilient Modulus [Mr]: Cyclic Loading, Composite, Stress-Dependent		
Project Name:	18 El Centro, CA	
Project ID:	Tensar	
Location:	Interstate 8, East Bound, East of Bonds Corner Rd.	

Automated Plate Load Test [APLT]

Test:	In-situ Resilient Modulus [Mr]: Cyclic Loading, Composite, Stress-Dependent (5, 10, 15, 20, 30, 40)				
Date:	5/9/2016	Time:	6:39:30 PM	Test ID:	I-8_sta2726
Tested By:	DW, HG	Location:	East Bound- Center	Sta.:	2726
Latitude:	32.773232	Longitude:	115.328090	Elev. (m):	1.26
Comments:	Recycled aggregate base (0.55 ft) stabilized with TX160 geogrid. Plate size correction ($F_{corrected}$) = 1.00.				

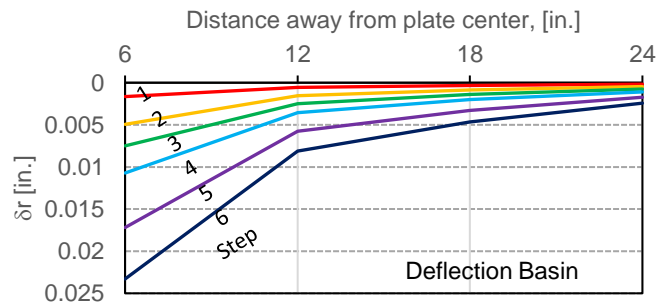
Step	N	$\sigma_{cyclic_surface}$ [psi]	M_{r-Base} [psi]	M_{r-Base} (pred.) [psi]	$\sigma_{cyclic_Int.}$ [psi]	$M_{r-Subgrade}$ [psi]	$M_{r-Subgrade}$ (pred.) [psi]	Modulus Ratio
Conditioning	500	13.92	---	---	---	---	---	---
1	100	3.83	68,850	---	1.55	18,434	18,411	3.73
2	100	9.20	49,147	49,689	4.00	15,836	15,784	3.10
3	100	13.92	55,388	52,665	5.64	14,745	14,899	3.76
4	100	19.08	53,376	54,178	7.73	14,115	14,145	3.78
5	100	29.62	52,806	54,673	11.80	13,500	13,241	3.91
6	100	39.03	54,938	53,785	14.97	12,650	12,795	4.34



Model: AASHTO (2015)

$$M_r = k_1^* P_a \left(\frac{\theta}{P_a} \right)^{k_2^*} \left(1 + \frac{\tau_{occl}}{P_a} \right)^{k_3^*}$$

Parameter	Value	P-Value
k_1^* (Base)	3425.7	2.41E-07
k_2^* (Base)	0.277	2.30E-01
k_3^* (Base)	-1.262	3.24E-01
Adj. R^2	0.553	
Std. Error [psi]	1495	
k_1^* (Subgrade)	952.4	5.41E-07
k_2^* (Subgrade)	-0.214	7.36E-03
k_3^* (Subgrade)	0.377	3.77E-01
Adj. R^2	0.993	
Std. Error [psi]	169	

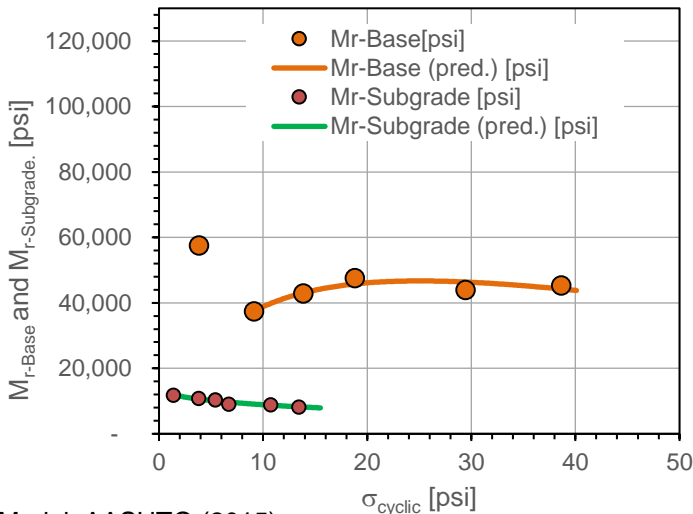


In-situ Resilient Modulus [Mr]: Cyclic Loading, Layered Analysis, Stress-Dependent		
Project Name:	18 El Centro, CA	
Project ID:	Tensar	
Location:	Interstate 8, East Bound, East of Bonds Corner Rd.	

Automated Plate Load Test [APLT]

Test:	In-situ Resilient Modulus [Mr]: Cyclic Loading, Composite, Stress-Dependent (5, 10, 15, 20, 30, 40)				
Date:	5/9/2016	Time:	7:16:18 PM	Test ID	I-8_sta2729
Tested By	DW, HG	Location:	East Bound- Center	Sta.	2729
Latitude:	32.773228	Longitude,W:	115.327120	Elev. (m):	1.54
Comments:	Recycled aggregate base (0.55 ft) stabilized with TX160 geogrid. Plate size correction ($F_{corrected}$) = 1.00.				

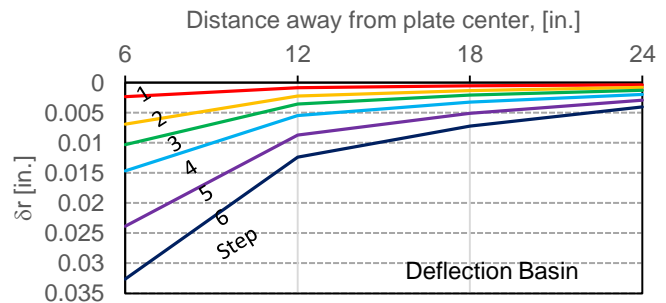
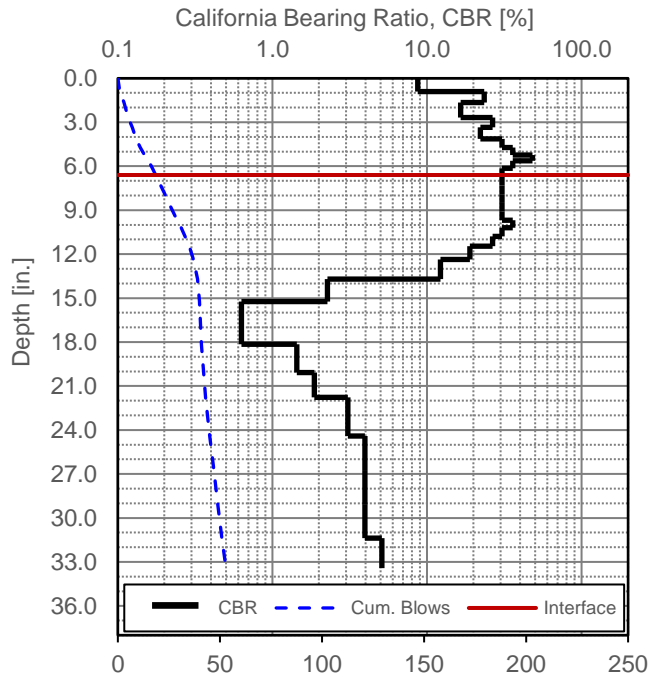
Step	N	$\sigma_{cyclic_surface}$ [psi]	M_{r-Base} [psi]	M_{r-Base} (pred.) [psi]	$\sigma_{cyclic_Int.}$ [psi]	$M_{r-Subgrade}$ [psi]	$M_{r-Subgrade}$ (pred.) [psi]	Modulus Ratio
Conditioning	500	13.87	---	---	---	---	---	---
1	100	3.83	57,549	---	1.40	11,851	11,946	4.86
2	100	9.14	37,441	37,565	3.81	10,879	10,606	3.44
3	100	13.87	42,885	43,047	5.43	10,304	10,031	4.16
4	100	18.81	47,584	45,770	6.69	9,076	9,661	5.24
5	100	29.44	43,955	46,372	10.73	8,920	8,735	4.93
6	100	38.63	45,379	44,255	13.44	8,224	8,246	5.52



Model: AASHTO (2015)

$$M_r = k_1^* P_a \left(\frac{\theta}{P_a}\right)^{k_2^*} \left(1 + \frac{\tau_{ocf}}{P_a}\right)^{k_3^*}$$

Parameter	Value	P-Value
k_1^* (Base)	2677.5	3.10E-07
k_2^* (Base)	0.669	4.03E-02
k_3^* (Base)	-3.172	6.70E-02
Adj. R^2	0.851	
Std. Error [psi]	1523	
k_1^* (Subgrade)	732.8	2.03E-05
k_2^* (Subgrade)	-0.102	3.82E-01
k_3^* (Subgrade)	-1.051	4.48E-01
Adj. R^2	0.929	
Std. Error [psi]	355	

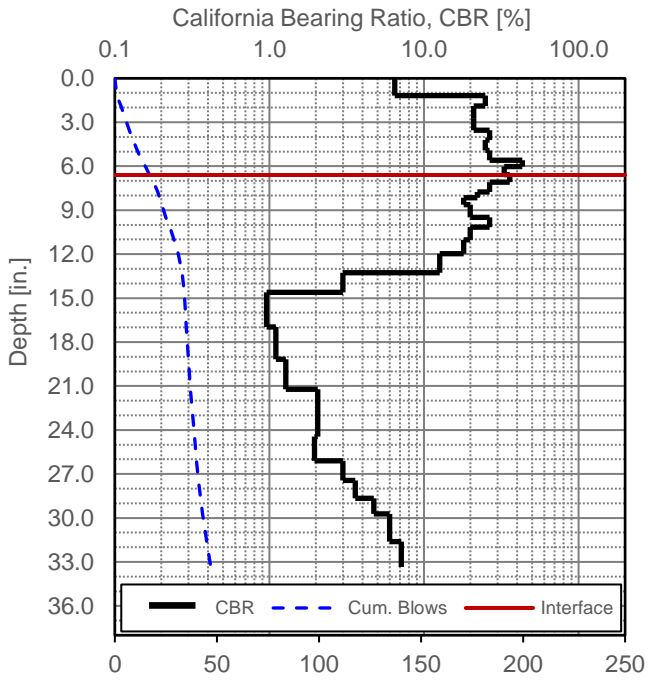
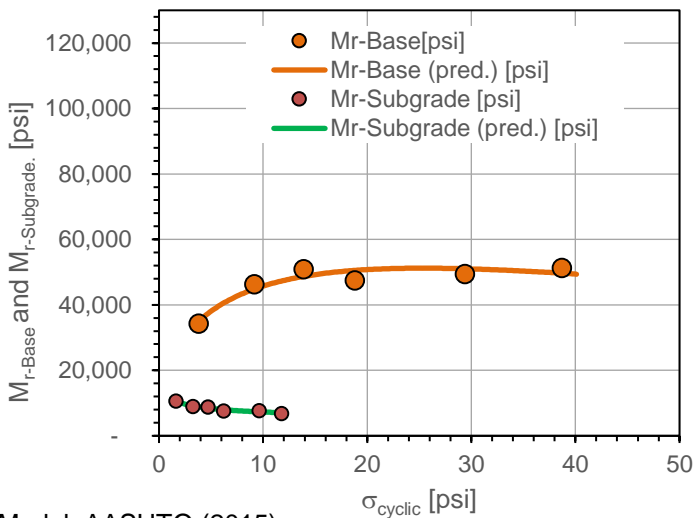


In-situ Resilient Modulus [Mr]: Cyclic Loading, Layered Analysis, Stress-Dependent		
Project Name:	18 El Centro, CA	
Project ID:	Tensar	
Location:	Interstate 8, East Bound, East of Bonds Corner Rd.	

Automated Plate Load Test [APLT]

Test:	In-situ Resilient Modulus [Mr]: Cyclic Loading, Composite, Stress-Dependent (5, 10, 15, 20, 30, 40)				
Date:	5/9/2016	Time:	7:54:11 PM	Test ID	I-8_sta2732
Tested By	DW, HG	Location:	East Bound- Center	Sta.	2732
Latitude:	32.773216	Longitude:	115.326140	Elev. (m):	0.04
Comments:	Recycled aggregate base (0.55 ft) stabilized with TX160 geogrid. Plate size correction ($F_{corrected}$) = 1.00.				

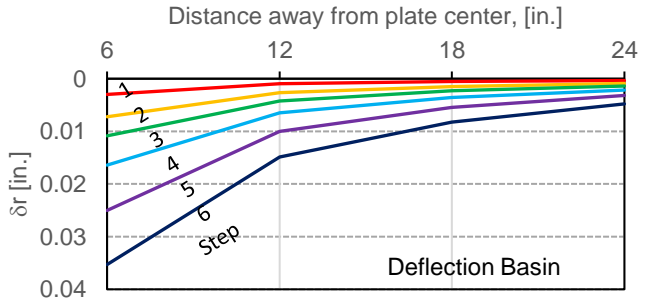
Step	N	$\sigma_{cyclic_surface}$ [psi]	M_{r-Base} [psi]	M_{r-Base} (pred.) [psi]	$\sigma_{cyclic_Int.}$ [psi]	$M_{r-Subgrade}$ [psi]	$M_{r-Subgrade}$ (pred.) [psi]	Modulus Ratio
Conditioning	500	13.88	---	---	---	---	---	---
1	100	3.80	34,262	34,867	1.63	10,660	10,593	3.21
2	100	9.15	46,328	44,833	3.26	8,984	9,143	5.16
3	100	13.88	50,964	48,679	4.72	8,692	8,442	5.86
4	100	18.80	47,470	50,534	6.21	7,624	7,967	6.23
5	100	29.40	49,471	51,033	9.62	7,757	7,321	6.38
6	100	38.69	51,326	49,686	11.78	6,848	7,071	7.49



Model: AASHTO (2015)

$$M_r = k_1^* P_a \left(\frac{\theta}{P_a} \right)^{k_2^*} \left(1 + \frac{\tau_{ocf}}{P_a} \right)^{k_3^*}$$

Parameter	Value	P-Value
k_1^* (Base)	3129.4	1.00E-06
k_2^* (Base)	0.400	2.97E-02
k_3^* (Base)	-1.875	8.86E-02
Adj. R^2	0.863	
Std. Error [psi]	2280	
k_1^* (Subgrade)	494.7	8.29E-05
k_2^* (Subgrade)	-0.296	1.45E-01
k_3^* (Subgrade)	0.812	6.95E-01
Adj. R^2	0.937	
Std. Error [psi]	326	



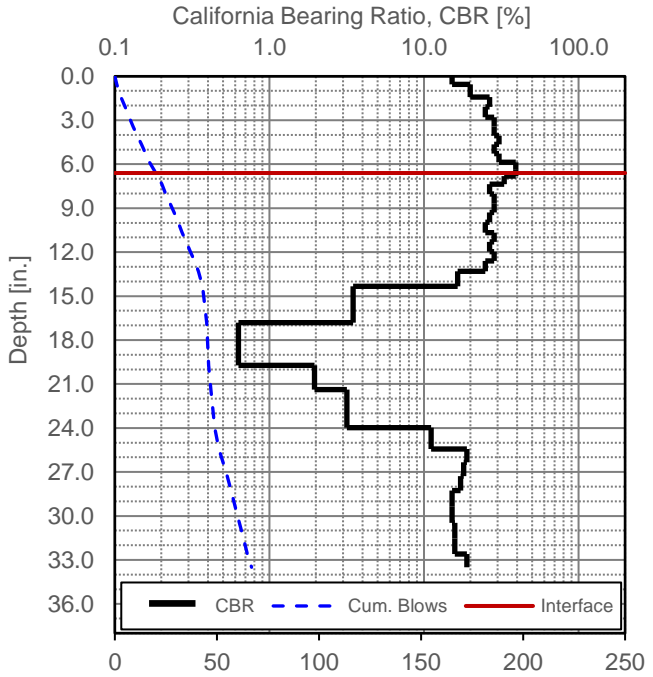
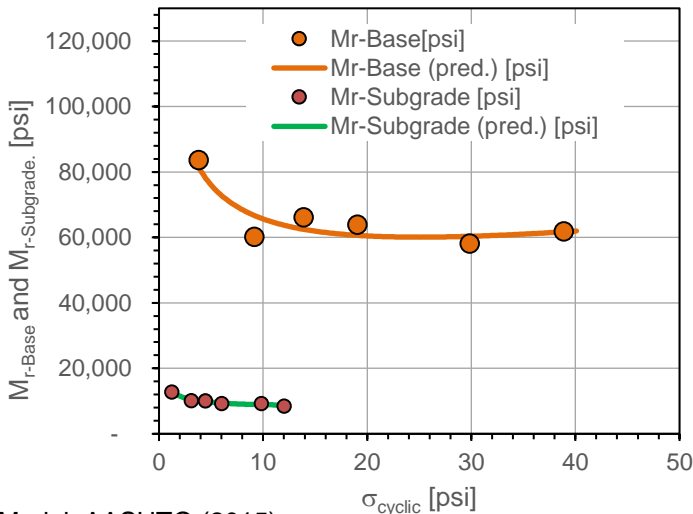
In-situ Resilient Modulus [Mr]: Cyclic Loading, Layered Analysis, Stress-Dependent	
Project Name:	18 El Centro, CA
Project ID:	Tensar
Location:	Interstate 8, East Bound, East of Bonds Corner Rd.



Automated Plate Load Test [APLT]

Test:	In-situ Resilient Modulus [Mr]: Cyclic Loading, Composite, Stress-Dependent (5, 10, 15, 20, 30, 40)				
Date:	5/9/2016	Time:	8:29:43 PM	Test ID:	I-8_sta2738_50
Tested By:	DW, HG	Location:	East Bound- Center	Sta.:	2738_50
Latitude:	32.773216	Longitude:	115.324020	Elev. (m):	3.61
Comments:	Recycled aggregate base (0.55 ft) stabilized with TX160 geogrid. Plate size correction ($F_{corrected}$) = 1.00.				

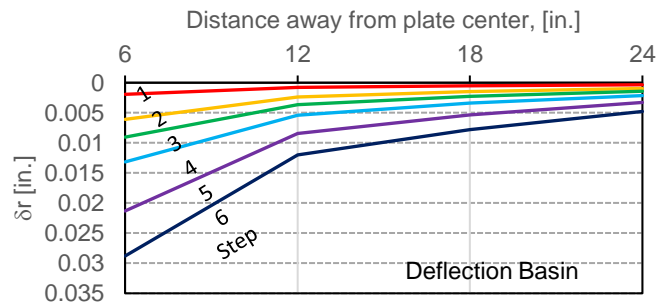
Step	N	$\sigma_{cyclic_surface}$ [psi]	M_{r-Base} [psi]	M_{r-Base} (pred.) [psi]	$\sigma_{cyclic_Int.}$ [psi]	$M_{r-Subgrade}$ [psi]	$M_{r-Subgrade}$ (pred.) [psi]	Modulus Ratio
Conditioning	500	13.88	---	---	---	---	---	---
1	100	3.80	83,675	81,531	1.23	12,797	12,651	6.54
2	100	9.16	60,256	66,683	3.11	10,183	10,526	5.92
3	100	13.88	66,140	62,487	4.47	9,998	9,842	6.62
4	100	19.05	63,901	60,633	6.02	9,316	9,387	6.86
5	100	29.84	58,128	60,335	9.84	9,312	8,891	6.24
6	100	38.87	61,914	61,707	12.00	8,519	8,804	7.27



Model: AASHTO (2015)

$$M_r = k_1^* P_a \left(\frac{\theta}{P_a} \right)^{k_2^*} \left(1 + \frac{\tau_{oct}}{P_a} \right)^{k_3^*}$$

Parameter	Value	P-Value
k_1^* (Base)	4438.4	2.37E-06
k_2^* (Base)	-0.321	1.10E-01
k_3^* (Base)	1.518	2.42E-01
Adj. R^2	0.782	
Std. Error [psi]	3802	
k_1^* (Subgrade)	524.0	2.35E-05
k_2^* (Subgrade)	-0.323	4.13E-02
k_3^* (Subgrade)	1.869	2.26E-01
Adj. R^2	0.952	
Std. Error [psi]	316	

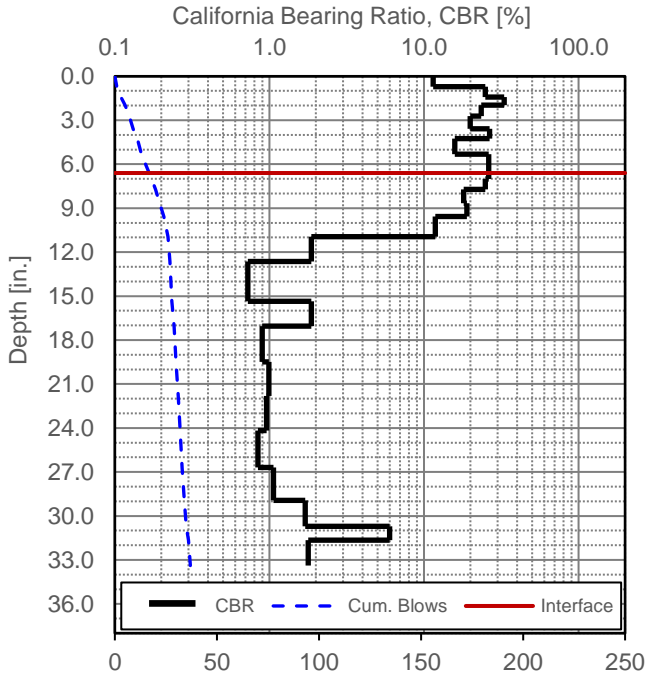
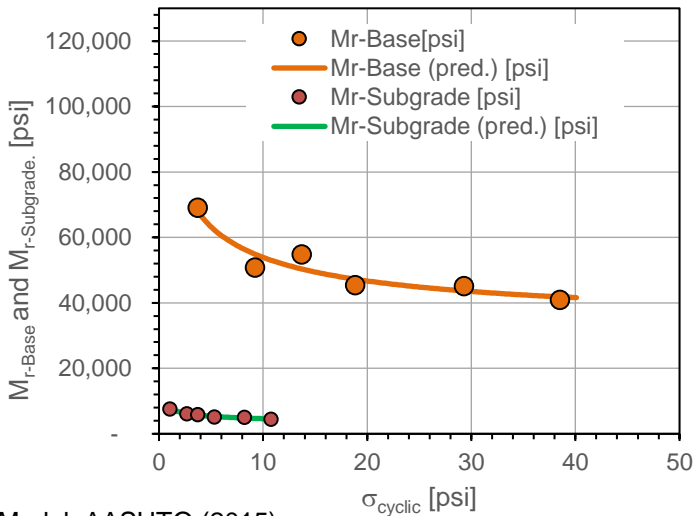


In-situ Resilient Modulus [Mr]: Cyclic Loading, Layered Analysis, Stress-Dependent		
Project Name:	18 El Centro, CA	
Project ID:	Tensar	
Location:	Interstate 8, East Bound, East of Bonds Corner Rd.	

Automated Plate Load Test [APLT]

Test:	In-situ Resilient Modulus [Mr]: Cyclic Loading, Composite, Stress-Dependent (5, 10, 15, 20, 30, 40)				
Date:	5/9/2016	Time:	9:07:28 PM	Test ID:	I-8_sta2747_50
Tested By:	DW, HG	Location:	East Bound- Center	Sta.:	2747_50
Latitude:	32.773201	Longitude:	115.321090	Elev. (m):	1.75
Comments:	Recycled aggregate base (0.55 ft) stabilized with TX160 geogrid. Plate size correction ($F_{corrected}$) = 1.00.				

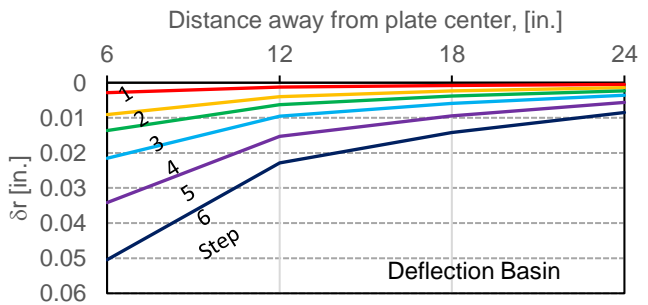
Step	N	$\sigma_{cyclic_surface}$ [psi]	M_{r-Base} [psi]	M_{r-Base} (pred.) [psi]	$\sigma_{cyclic_Int.}$ [psi]	$M_{r-Subgrade}$ [psi]	$M_{r-Subgrade}$ (pred.) [psi]	Modulus Ratio
Conditioning	500	13.70	---	---	---	---	---	---
1	100	3.72	69,081	67,931	1.03	7,658	7,607	9.02
2	100	9.22	50,831	54,875	2.67	6,117	6,210	8.31
3	100	13.70	54,855	50,365	3.74	5,795	5,746	9.47
4	100	18.84	45,456	47,238	5.32	5,181	5,297	8.77
5	100	29.30	45,175	43,643	8.20	5,042	4,813	8.96
6	100	38.50	40,946	41,844	10.75	4,444	4,554	9.21



Model: AASHTO (2015)

$$M_r = k_1^* P_a \left(\frac{\theta}{P_a} \right)^{k_2^*} \left(1 + \frac{\tau_{occl}}{P_a} \right)^{k_3^*}$$

Parameter	Value	P-Value
k_1^* (Base)	3969.3	2.17E-06
k_2^* (Base)	-0.259	1.48E-01
k_3^* (Base)	0.397	7.16E-01
Adj. R^2	0.891	
Std. Error [psi]	3140	
k_1^* (Subgrade)	320.6	2.35E-05
k_2^* (Subgrade)	-0.307	3.18E-02
k_3^* (Subgrade)	0.706	5.91E-01
Adj. R^2	0.982	
Std. Error [psi]	150	

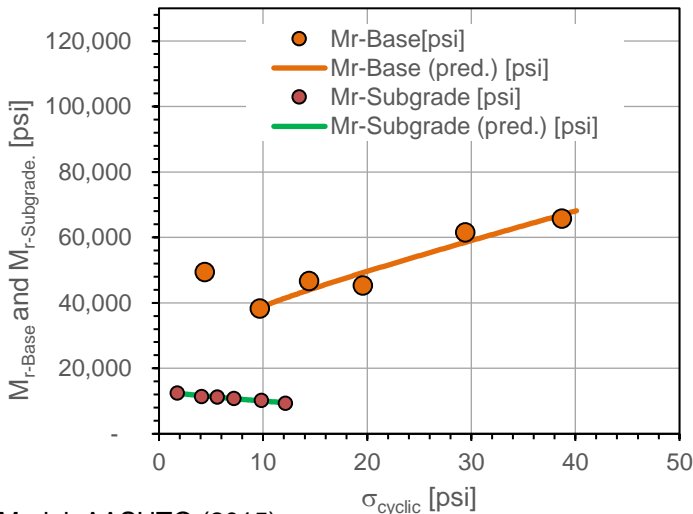


In-situ Resilient Modulus [Mr]: Cyclic Loading, Layered Analysis, Stress-Dependent		
Project Name:	18 El Centro, CA	
Project ID:	Tensar	
Location:	Interstate 8, East Bound, East of Bonds Corner Rd.	

Automated Plate Load Test [APLT]

Test:	In-situ Resilient Modulus [Mr]: Cyclic Loading, Composite, Stress-Dependent (5, 10, 15, 20, 30, 40)				
Date:	5/10/2016	Time:	11:30:55 AM	Test ID	18 2756 50
Tested By	DW, HG	Location:	East Bound- Center	Sta.	2756_50
Latitude:	32.773178	Longitude,W:	115.318180	Elev. (m):	8.20
Comments:	Recycled aggregate base (0.55 ft) stabilized with TX160 geogrid. Plate size correction ($F_{corrected}$) = 1.00.				

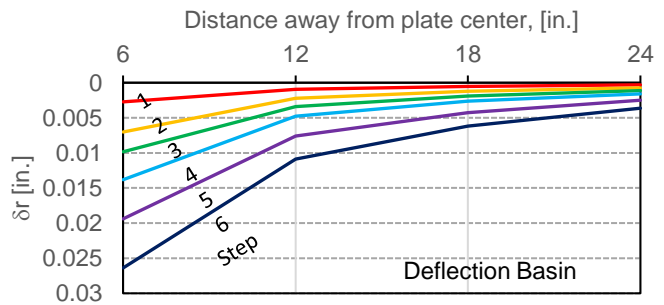
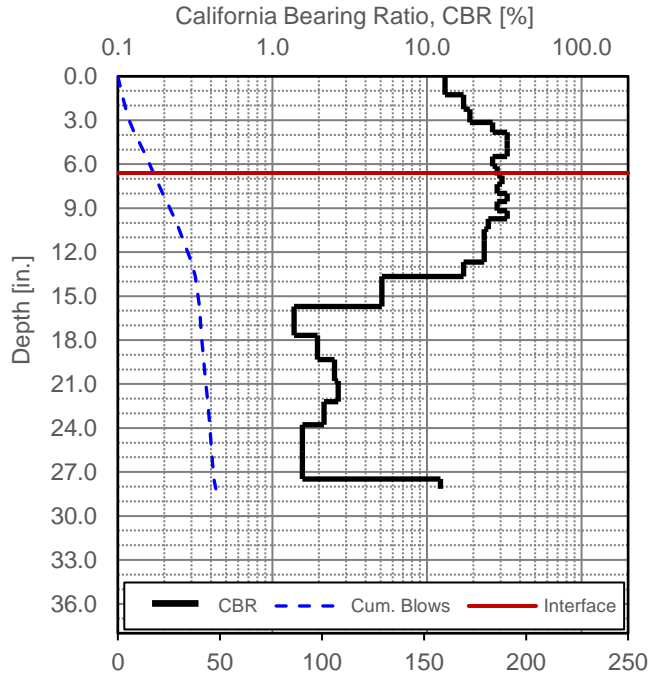
Step	N	$\sigma_{cyclic_surface}$ [psi]	M_{r-Base} [psi]	M_{r-Base} (pred.) [psi]	$\sigma_{cyclic_Int.}$ [psi]	$M_{r-Subgrade}$ [psi]	$M_{r-Subgrade}$ (pred.) [psi]	Modulus Ratio
Conditioning	500	14.40	---	---	---	---	---	---
1	100	4.39	49,459	---	1.75	12,495	12,413	3.96
2	100	9.68	38,362	38,614	4.10	11,399	11,643	3.37
3	100	14.40	46,689	43,944	5.62	11,218	11,184	4.16
4	100	19.58	45,338	49,210	7.20	10,838	10,736	4.18
5	100	29.42	61,588	58,497	9.85	10,209	10,044	6.03
6	100	38.70	65,771	66,899	12.13	9,369	9,503	7.02



Model: AASHTO (2015)

$$M_r = k_1^* P_a \left(\frac{\theta}{P_a}\right)^{k_2^*} \left(1 + \frac{\tau_{ocf}}{P_a}\right)^{k_3^*}$$

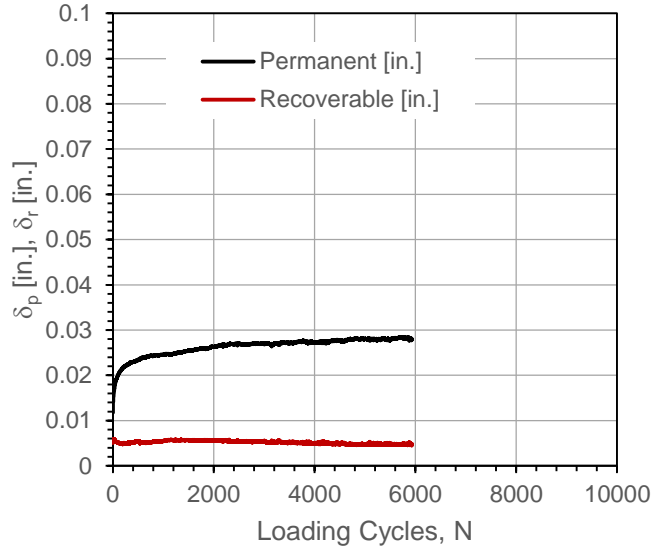
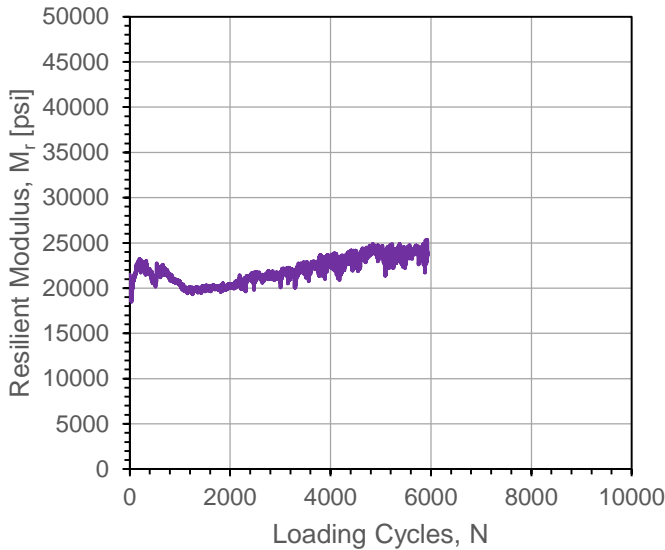
Parameter	Value	P-Value
k_1^* (Base)	2164.2	1.40E-06
k_2^* (Base)	0.204	5.90E-01
k_3^* (Base)	1.076	6.19E-01
Adj. R^2	0.939	
Std. Error [psi]	2822	
k_1^* (Subgrade)	898.9	3.17E-06
k_2^* (Subgrade)	-0.001	9.86E-01
k_3^* (Subgrade)	-1.915	7.01E-02
Adj. R^2	0.973	
Std. Error [psi]	174	



In-situ Resilient Modulus [Mr]: Cyclic Loading, Layered Analysis, Stress-Dependent		
Project Name:	18 El Centro, CA	
Project ID:	Tensar	
Location:	Interstate 8, East Bound, East of Bonds Corner Rd.	

Automated Plate Load Test [APLT]

Test:	In-situ Resilient Modulus [Mr]: Cyclic Loading, 6,000 cycles, Composite [Cyclic Stress = 10 psi]				
Date:	5/10/2016	Time:	2:40:17 PM	Test ID	I8_Extended_10psi
Tested By	DW, HG	Location:	East Bound- Center	Sta.	2732+00
Latitude:	32.773213	Longitude:	115.326180	Elev. (m):	-0.4
Comments:	Recycled aggregate base (0.55 ft) stabilized with TX160 geogrid. Plate size correction ($F_{corrected}$) = 1.00.				



$M_{r-comp} =$ 23,890 psi [Average of the last 10 cycles]
 $\sigma_{cyclic} =$ 8.5 psi

Permanent Deformation Prediction Parameters

$C =$ 0.0137
 $d =$ 0.0842
 $R^2 =$ 0.9790

$N^* =$ 2,209 Cycles
 $\delta_p \text{ at } N^* =$ 0.0262 in.
 Adj. $\delta_p \text{ at } N^* =$ 0.0125 in.

$N_{0.05} =$ 4,688,705 Cycles
 $N_{0.1} =$ >>10,000,000 Cycles
 $N_{0.15} =$ >>10,000,000 Cycles
 $N_{0.20} =$ >>10,000,000 Cycles
 $N_{0.25} =$ >>10,000,000 Cycles
 $N_{0.30} =$ >>10,000,000 Cycles
 $N_{0.40} =$ >>10,000,000 Cycles
 $N_{0.50} =$ >>10,000,000 Cycles

Model: $\delta_p = CN^d$

δ_p = permanent deformation
 C = plastic deformation after first cycle
 d = scaling component
 N = Number of loading cycles
 N^* = Number of loading cycles at $\Delta\delta_p = 1E-06$ in./cycles
 Adj. $\delta_p \text{ at } N^* = \delta_p \text{ at } N^* - C$
 N_x = Number of loading cycles to achieve δ_p of x in.

In-situ Resilient Modulus [Mr] and Permanent Deformation [delta_p]: Cyclic Loading

Project Name: I8 El Centro, CA
 Project ID: Tensar
 Location: Interstate 8, East Bound, East of Bonds Corner Rd.

